Emerging Techniques for Fabrication of Hydrophobic and Super-Hydrophobic Substrate: A Review

Tushar Gupta[a], Basant Singh Sikarwar[a*], Mukesh Ranjan[b] and Devesh Kumar Avasthi[c*]

[a]Department of Mechanical Engineering, Amity University UP, NOIDA

[b] Institute of Plasma Research, Ahmedabad India

[c] UPES, Dehradun India

*Corresponding author:
bssikarwar@amity.edu
dka4444@gmail.com

Abstract: *Recent advances in nanotechnology, chemical/physical texturing, and thin-film coating technology generate definite possibilities for the fabrication of super-hydrophobic metallic durable substrate which having low contact angle hysteresis. Availability of superior experimental techniques also leads to a deeper understanding of the process parameters controlling the relevant physics for quantifying the surface hydrophobicity, the distinguishing feature of which is the involvement of a hierarchy of length scales like length-scale of roughness in lotus leaf.* In this review paper, a holistic view of the complete hierarchy of the *processes involved in the fabrication of metallic superhydrophobic surfaces by various processes was reviewed. The state-of-the-art on the subject has been scrutinized based on (a) Basic concepts and physics of superhydrophobic surfaces, (b) Methods and Materials for metallic superhydrophobic fabrication, (c) advancement of ion beam radiation and plasma process for fabrication of superhydrophobic metallic substrate and (d) finally, its application for enhancement transport coefficients of moist air condensation were reported.*

Keywords: Chemical coating, Plasma process, Ion beam irradiation, Physical texturing, chemical texturing, hydrophobicity, Moist air Condensation

Contents:

1. **Introduction:** What are super-hydrophobic surfaces? & their applications in engineering
2. **Basic concepts and physics of superhydrophobic surfaces**
    - Lotus Effect
    - Contact Angle Hysteresis
    - Wenzel Model
    - Cassie-Baxter Model

3. **Methods and Materials**
   Superhydrophobic surfaces creation by Chemical Etching & Coating
    - Chemical Process
    - Physical Process
    - Combination of both
4. **Plasma process for superhydrophobic surfaces**
   Creation of Plasma, DC Plasma Discharge, DC Magnetron Discharge, RF Plasma Discharge, RF Magnetron Discharge, AC Plasma Sputtering, Chemical Vapor Deposition, Plasma Laser Processing, Ion beam irradiation
5. Summary & Conclusion
6. References

1. Introduction:

A water droplet placed on the hydrophilic surface forms a water film and it forms a spherical-cap shape drop on the hydrophobic surface[1]. This happens because of the balance of various interface energy as shown in Figure 1. Thomas Young[2] expressed the relationship with various interface energies for a stationary droplet.

$$\cos\theta = \frac{\sigma_{sl} - \sigma_{sv}}{\sigma_{lv}} \qquad (1)$$

Here, θ is the contact angle between the liquid-vapor interface ad solid-liquid interface of a drop, as shown in Figure 1. It depends on the various interface energies. High surface energy has a small value of contact angle, and these are known as hydrophilic surfaces. Small surface energy has a large value of contact angle and these are known as hydrophobic surfaces. Hence, the contact angle quantifies the surface hydrophobicity of the liquid of droplet, as shown in Figure 2. Hydrophilic surfaces have contact angles of water droplets less than 90°. However, the hydrophobic surfaces have an angle greater than 90° and the super-hydrophobic surfaces have a contact angle of more than 150° [3].

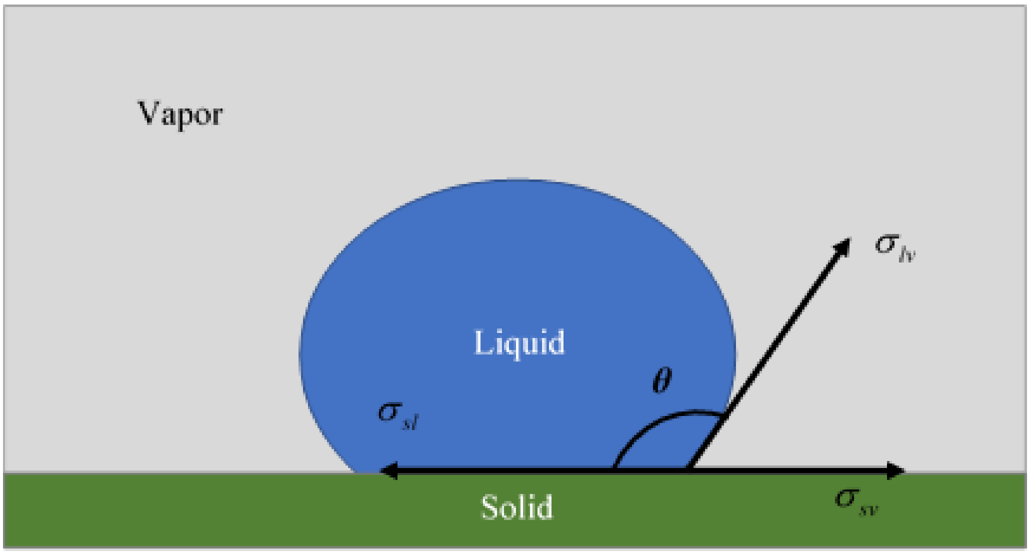

Figure 1: Representation of energy balances on the solid surface on the three-phase contact line

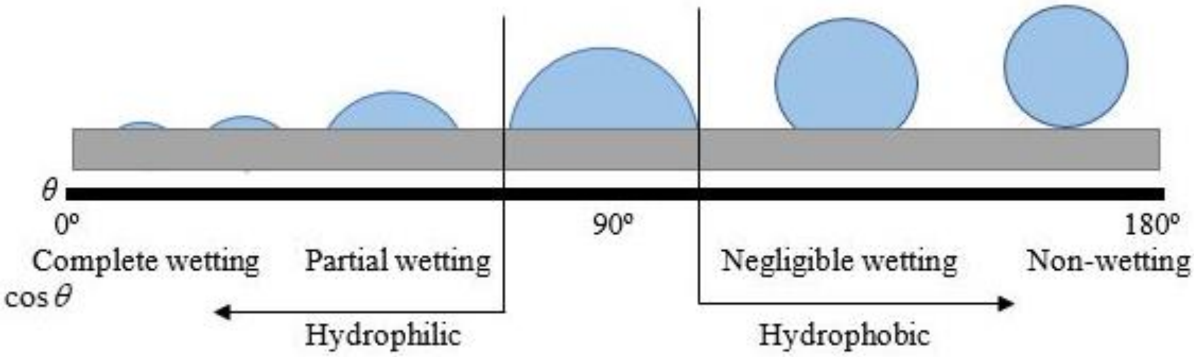

Figure 2:Schematic view of water droplets position on various wettability surfaces

Superhydrophobic surfaces have tremendous applications in manufacturing industries, automobile sector[4], medical equipment[5], marine industries[6], oil-water separation[7], corrosion-resistant surfaces[8], anti-icing surface[9], reducing the drag force [10] and two-phase processes. Condensation and evaporation prefer on the super-hydrophobic surface because of transport coefficients (mass transfer and heat transfer coefficient) of these processes are at least one order higher than the hydrophilic surfaces [11]. In this way, superhydrophobic surfaces save energy and material for many thermal engineering process applications [12]. Consequently, a two-phase process on/underneath metallic substrate is widely used in the cooling of electronic components, energy storage, water harvesting from moist air, power cycle, and thermal management of the building. In nature, the metallic substrate has higher thermal conductivity and higher surface energy. In literature [13–18], many methods are reported for altering the surface energy of the metallic substrate for enhancing the efficacy of the surface. These methods are categorized as chemical and physical texturing. These methods have their pros and cons for fabricating the superhydrophobic metallic surface. The major issues are as costly, tedious, durability, and droplet pinning phenomena [4]. Therefore, these surfaces are limited for deployment in many engineering systems[19].

In this paper, the state-of-the-art on the hydrophobic/superhydrophobic metallic substrates and their fabrication processes have been scrutinized. The subject matter has been arranged in the following sequence:

i. Introduction to metallic superhydrophobic substrates and their applications
ii. Super-hydrophobic metallic surfaces and their morphology were discussed concerning the contact angle and texturing theories associated with measuring the contact angle and contact hysteresis.

iii. Fabrication of hydrophobic/super-hydrophobic substrates along with novel and emerging techniques for enhancing the super-hydrophobicity of the surfaces by chemical etching, chemical and physical texturing

iv. Ion-beam irradiation and plasma processes for the fabrication of metallic substrates were discussed in detail along with their findings.

v. Finally, a review of the metallic superhydrophobic application for moist air condensation was explored.

2. Contact angle and its hysteresis measurement on textured substrates:

In many applications, Superhydrophobic surfaces having a contact angle above 150^{o} and its hysteresis (i.e., the difference between the advancing and receding angle) is less than 10^{o} is preferred [20]. . These surfaces repel the liquid droplets and at a small value of its hysteresis has high capability of self-cleaning property [21]. In nature, the lotus leaf is an ideal self-cleaning superhydrophobic surface. The lotus leaf is not a smooth surface and nano-order roughness superimposes micro-order roughness in it. In equation 1, the symbol θ is the contact angle for an ideally smooth substrate with has no chemical heterogeneities. Real superhydrophobic substrates depart from an ideal behavior since they are not perfectly smooth substrates. In chemical coating super-hydrophobic substates, their composition may also vary slightly with the location. Molecules, atoms, or ions of other chemical species may be adsorbed on the substrate. Similarly, nano-order roughness is generated for the fabrication of super-hydrophobic substrates in physical texturing substrates. Effectively, the static contact angle turns out to be non-unique on the real substrate and can only be experimentally determined. The experimentally observed contact angle depends on the way the surface was prepared. De Gennes [22] and Leger [23] have shown that a wetting experiment is extremely sensitive to heterogeneities of the solid substrate. One of the first attempts at understanding the influence of roughness on wetting is due to Wenzel [24] who proposed the relationship following for the apparent contact angle. Against this background, this section elaborates the contact and its hysteresis measurements on real hydrophobic/superhydrophobic substrates.

Lotus Effect: The lotus effect refers to the property of the lotus leaves which involves two most important factors i.e. Superhydrophobicity and self-cleaning. The lotus leaf surface was cleaned by the dew drops, rainwater and these drops carried away the dust particles from the surface because of the surface roughness introduced between the contact area of the droplet with the leaf surface which reduces the adhesion between them and this roughness introduced because of epicuticular wax crystals[25]. It is shown that the factors affecting the self-cleaning property of natural superhydrophobic surfaces were water repellency, surface roughness, and reduced particle adhesion. It has been reported that many natural plants and animals possess water-repellency due to hydrophobic surfaces with microscopic roughness which causes anti-adhesive property against the surface contamination[26].

In lotus Leaf, because of the nano-structures surfaces present on their surface and coated with hydrophobic wax which makes the surface quite rough at the nanoscale which resulted in a hydrophobic surface[26]. This epicuticular wax contains non-methyl polar groups (CH_3) at the surface which discourages the leaf-water interaction because of the polar nature of water so the lotus effect is the result of the rough structure of the leaf and the non-polar wax which makes the surface water repellent and roll on the surface easily[27] Since the contact area reduced between the water droplets and leaf surface which increased static contact angle greater than 150° and when the surface was titled with slight angle water droplets rolls on the surface and carried the dirt particles present on it as demonstrated in Figure 3.

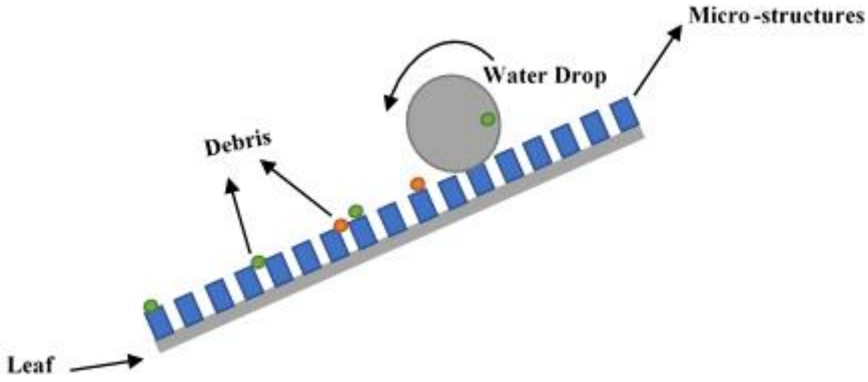

Figure 3: Illustration of Lotus Effect, water drop carried the dirt particles while rolling on the surface.

The contact angle measurement is one of the effective techniques for understanding the three-phase surface interactions (solid/liquid/air). The relationship between contact and the surface tension obtained by Young’s equation [28] as mentioned above and is based on the assumptions that the surface should be rigid, flat, homogeneous, and nonporous which was referred to as the ideal surface.

Wetting is the property of a liquid droplet for maintaining contact with the solid surface, depending upon the contact angle of a droplet with the surface. As it is discussed in the literature [29] that the hydrophilic, hydrophobic, and superhydrophobic surfaces differentiated by the contact angle i.e. $\theta < 90^\circ$, $90^\circ < \theta < 150^\circ$, and $\theta > 150^\circ$, respectively. The degree of wetting which is termed as wettability represents the affinity of the droplet with the surface due to the cohesive and adhesive forces.

Contact Angle Hysteresis: Young's equation is mostly applicable for static contact angle related to three interfacial surface tensions like σ_{SV} - solid vapor, σ_{SL} - solid-liquid & σ_{LV} - liquid-vapor. But as discussed in literature there is the existence of non-ideal surface heterogeneity which led to the formation of contact angles which is not equal to a single value of static contact angle. The wetting phenomenon is not just a static state, but it is a dynamic state in which the three interfacial surface tensions are in motion and the contact angle formed on the surface is termed as dynamic contact angle[30].

Contact angle hysteresis is the most crucial factor in wetting of the liquid droplets on the surfaces, it can be very well understood by analyzing droplet on a vertical surface as shown in Figure 4 like the rain droplets falls on the window glass. Due to gravity, the drop tends to move down but because of contact angle hysteresis drop will remain on the vertical window glass due to which the angle made by the drop on the glass will be asymmetric. The top contact angle will be less due to which drop becomes thin while the bottom contact angle will be more due to which drop becomes thick. After a certain period, the drop will slide down, and the difference between the bottom contact angle (Advancing angle) and top contact angle (Receding angle) is called contact angle hysteresis[30].

The CAH is the difference between advancing angle and contact angle and it can be represented by the equation[31] :

$$\mathrm{H} = \theta_a - \theta_r \tag{2}$$

It is generalized for a non-ideal surface that the advancing angle represents low-wettability characteristics whereas the receding angle represents high-wettability characteristics[32]. Therefore, it is important to compute both the angles while doing contact angle measurements.

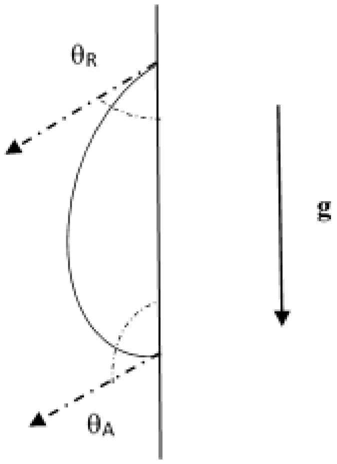

Figure 4: Representation of drop on the vertical substrate, as due to gravity the drops tends to move downward but CAH kept the droplet at a place such that the upper part of droplet becomes thin and the lower part becomes thick with advancing θ_A and receding angle θ_R

Surface roughness and surface chemistry are important parameters that affect the contact angle of the water droplet on the solid substrate, to describe these parameters two models have elaborated and modified Young's equation, one is the Wenzel model and another one is the Cassie-Baxter model.

2.3 Wenzel Model:

In 1936 Wenzel gave the model which depicts the static contact angle on a heterogeneous surface. As per his research, the surface roughness of the substrate had a greater influence on static contact angle[1]. In the Wenzel state, the liquid drop penetrates through the micro-structured grooves on the rough solid surface.

Wenzel modified Young's equation by introducing the roughness factor (r) i.e.

$$\cos\theta_w = r\left(\frac{\sigma_{SV}-\sigma_{SL}}{\sigma_{LV}}\right) = r\cos\theta \tag{3}$$

where **θ** is a generalization of Young's contact angle, **θ_W** is the Wenzel contact angle, and **r** is the roughness parameter which must be greater than unity, increase in the roughness factor lead increase in the contact angle of hydrophobic surface whereas a decrease in it leads to the decrease of contact angle in hydrophilic surfaces[29].

The Wenzel equation assumed that the liquid drop profile must be greater than the surface roughness scale and it completely penetrates the cavities, scratches on the solid surface[33] as shown in figure 5.

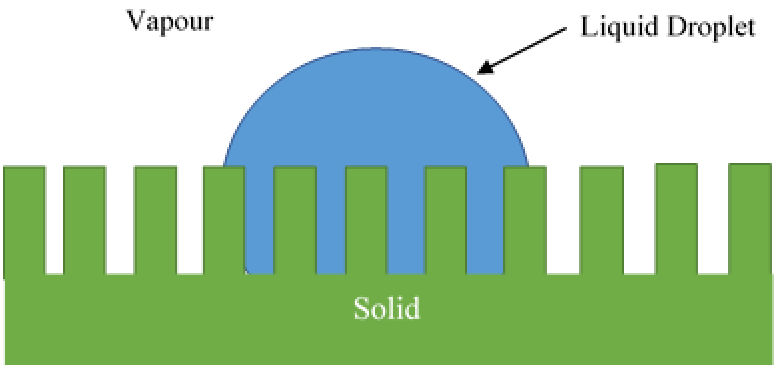

Figure 5: Wenzel Model Representation

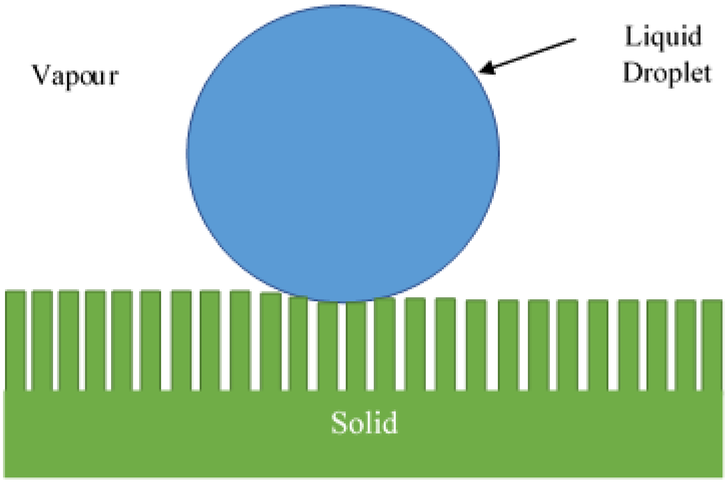

Figure 6: Cassie's Model Representation

Cassie-Baxter Model: As the surface is not ideal it would rather a heterogeneous surface so the relationship between the contact angle formed on the surface and the contact angle formed on the ideal surface discovered by the Cassie equation:

$$\cos\theta_c = f_1\cos(\theta_1) + f_2\cos(\theta_2) \tag{4}$$

where**θ_1** and **θ_2** are the contact angles for components 1 with fractional surface area f_1 and 2 with fractional surface area f_2 in the composite material, respectively.

This equation was derived in 1948 by Cassie while treating the Wenzel rough surface to be a heterogeneous surface. Cassie suggested a theory based on the above-mentioned equation that vapor of the liquid adsorbed on the solid surfaces when the contact angle assumed to be 0º and where it could not adsorb the contact angle assumed to be as close as 180º[33]. Contact angle hysteresis occurred due to heterogeneous surfaces, in which the advancing angle more closely related with the high contact angle regions whereas the receding angle with low contact angle regions[34] There are two sets of interfaces, one was the solid-liquid interface and the other was the composite interface which involved liquid-air and solid-air interfaces so for the calculation of the contact angle the Wenzel equation can be modified by combining the fractional surface area **f_1** which represents solid surface and fractional surface area **f_2** which represents air gaps such that the equation reduces to:

$$\cos\theta_c = f_1\cos\left(\theta_1\right) - f_2 \tag{5}$$

Different novel methods used for producing super-hydrophobic surface or super-hydrophobic coating on the metallic surfaces discussed further by discussing briefly the technology used for the process:

3. Methods and Materials

In nature, the metallic substrates are hydrophilic except noble metals. The metallic substrate was crafted hydrophobic/superhydrophobic by altering their surface morphology and coating by low surface energy materials. Fabrication of surfaces for creating micro/nanostructures on them so that they can be used effectively, and they can be made reliable from an industrial point of view. Generally, there are two methods used for altering the surface morphology, enhancing the wettability characteristics, and increasing the hydrophobicity on the surfaces are chemical texturing and physical texturing method.

Hydrophobicity of substrate depends on surface energy which is a strong function of surface morphologies. The substrate morphologies are crafted by chemical texturing and physical texturing in which micro/nanostructure roughness is formed effectively and efficiently so that substrate is reliable from an industrial point of view. Uniform, non-uniform micro/nano order roughness of substrate produces one order difference in substrate hydrophobicity. Dual order roughness morphology like a lotus leaf in which nano-order roughness superimposed on micro-order roughness prefer for a large value of hydrophobicity and small value of its hysteresis. So many chemical and physical texturing are broadly used in literature for altering the hydrophobicity of the surfaces, as shown in Figure 7. Details of these are given below.

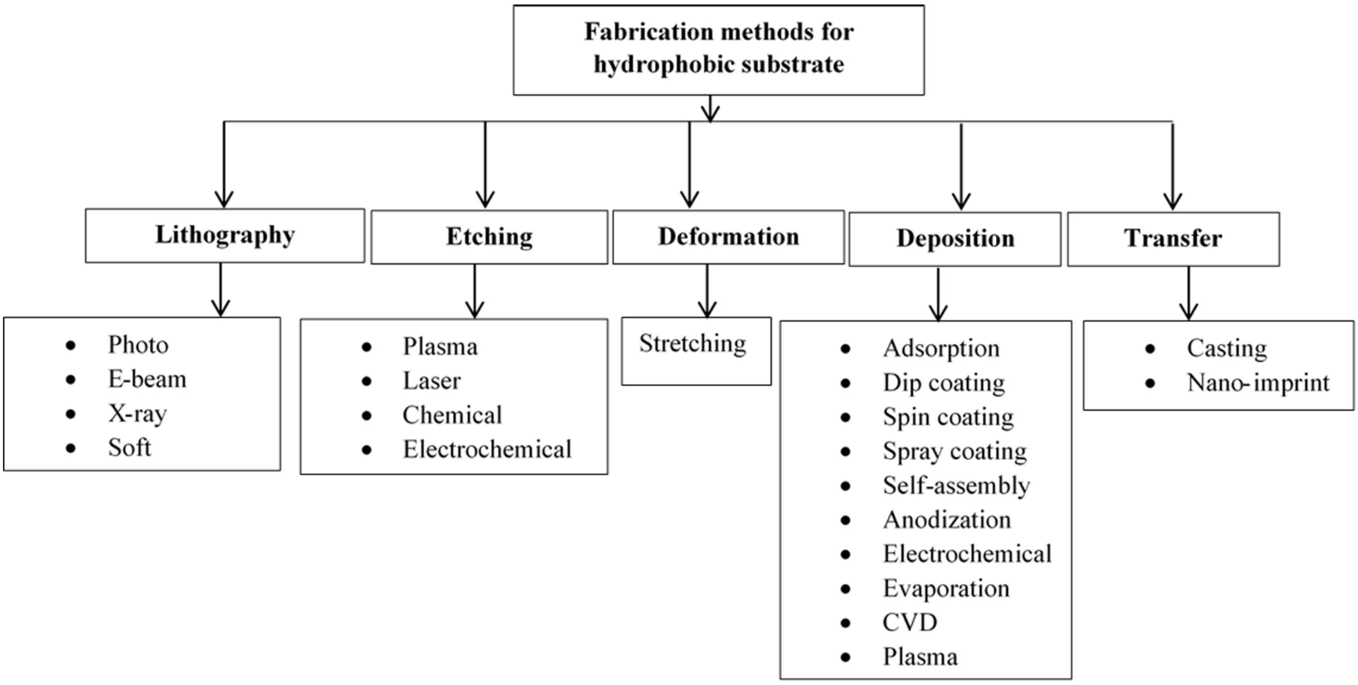

Figure 7: Various methods for fabrication of superhydrophobic substrate [35]**.**

3.1 Chemical Texturing:

In chemical texturing, various method of chemical etching, as well as the coating, is executed for altering the surface morphology. In chemical etching, the roughness is crafted by subtracting material by a chemical process. However, low energy material in micro-order is coated by the chemical process. Chemical coating and etching have their advantages and disadvantages.

In this technique, a coating is done on the substrate chemically with the organic compounds consisting of hydrophobic groups[36–39], inorganic compounds[40–43], polymers[44,45] and some special type of alloys[46,47]. The samples are dipped in the chemical solution at different speeds to obtain the required thickness of the film onto the substrate. After dip coating operation the samples were then annealed at a temperature in the range of 100 to 300 ºC for about ~ 10-30 minutes[48]. This process is very simple, but the surfaces created with the chemical texturing results in the degradation of the quality of the coating with time. The limitation of this technique can be overcome by using Ion-implantation which was successfully tested by many researchers[49–51].

The chemical etching and coating method for developing metallic superhydrophobic substrates have been discussed in detail:

Qian et al. [52] proposed a surface roughening method by simple chemical etching performed for the fabrication of superhydrophobic characteristics on aluminium, copper, and zinc, respectively. The aluminium samples were etched by immersing in Beck's dislocation etchant at a room temperature ~ 14ºC with the etching time varying from 5 to 15 seconds. Similarly, the copper and zinc substrates were etched using modified Livingston's dislocation etchant in a closed glass bottle at ambient temperature and using HCl solution in a glass beaker at room temperature. Contact angle over 150º with a roll of angle less than 10º reported by them.

Huang et al. [53] performed chemical etching on aluminium alloy 6061 using 1 M NaOH solution in an ultrasonic bath. Then the etched aluminium sample cleaned using distilled water and dried at 70ºC for more than 10 h. After that, the sample is immersed in 0.01 M ethanolic stearic acid solution. They have reported the improved corrosion-resistant properties and water contact angle of more than 150º investigated.

Liao et al. [54] fabricated the micro/nanostructured aluminium surfaces using the chemical etching method. The aluminium samples were washed using ethanol solution followed by distilled water and then immersing in 1 mol $CuCl_2$ solution for 8 seconds and further immersed in HCl acid for 10 seconds. The samples were then dissolved in 2 wt.% hexadecyltrimethoxysilane at ambient temperature for 60 min and heated at 90 ◦ C for 30 min. They reported the contact angle of 161.9º ± 0.5º and sliding angle of 6.8 ± 1º and improved the anti-icing property of the substrate.

Saleh et al. [55] fabricated the superhydrophobic stainless steel substrates for efficiently separating the non-polar organic components from water. Two-step process used for generating hydrophobic meshes. First, the stainless steel was cleaned with ethanol and washed with distilled water, and sonicated for 10 minutes to remove the dirt particles from the surface. Then, they are immersed in 25% sulphuric acid solution followed by immersing in 2% n-Octadecyltrichlorosilane solution. They have reported the contact angle of 166.8º and proved to be a valuable material for separating oil from the water.

Bahrami et al. [56] fabricated superhydrophobic copper surfaces using a chemical etching process. To remove the contaminants deposited on the copper specimen ultrasonically cleaned in an alkaline solution and then rinsed with deionized water, next to remove the copper oxides the specimen is dissolved in 5% sulphuric acid and then rinsed with DI water and dried at ambient temperature. Cleaned Cu plates etched by adding $FeCl_3$ to DI water and then stirring it and further dissolving in an ethanol solution of 10 mM stearic acid for 24 h and dried at ambient temperature. They reported a contact angle of more than 145º.

Wang et al. [17] performed electrochemical etching on Be-Cu alloy sheets of size 20 mm × 10 mm × 1 mm and block thickness of 50 mm. EDM machine with graphite tools as positive and substrate as the negative electrode, and kerosene is used as working fluid, discharge voltage set to 200 V with a duty ratio of 1:4, discharge current varied (12 A, 24 A, 36 A, 48 A, 60 A) to achieve micro-structured surface. Electrochemical etching was performed by making substrate as anode and graphite sheet as the cathode in 0.1 M HCL electrolyte with a voltage of 20 V for 2 min. Then after washing in ethanol solution the sample is immersed in 2 wt% stearic acid ethanol solution for 1 h, then dried under airflow. Water contact angle from 152.5 ± 2.3° to 167.1 ± 2.6° reported and sliding angle of 2.4 ± 0.7°.

Chen et al. [57] performed a chemical etching process on aluminium and zinc substrates. First, the samples were cleaned ultrasonically with ethanol, acetone, and deionized water and dried with the flow of nitrogen. 75 g stearic is added to the weighing bottle containing 20 ml water. Then the bottle was kept in a kettle containing water and the temperature was maintained at 75ºC for 15 minutes so that stearic acid got dissolve. Further 0.3 M HCL is added in the bottle and immediately the substrates dissolved in the solution for 15 min to 90 min for Al and 75 min for Zn. Then samples were cleaned in ethanol solution and dried heated airflow at 70ºC for 10 s. They reported the water contact angle of 150º and the rolling angle of 8º.

Varshney et al. [58] performed chemical etching on brass in a one and two-step process. First, the substrate is cleaned using Millipore water in ultra-sonicator for 10 min and then again cleaned in acetone solution and then dried at 40 ºC for 1 h. In a one-step process, the substrate is immersed in 20g/L ethanoic solution of lauric acid for 24 h and then rinsed with distilled water and dried for 24 h to obtain SH coating. In a two-step process, the substrate was immersed in a mixture of HNO3 and HCl for 60 min. which increases the surface roughness. After cleaning with distilled water and ethanol for 60 min the substrate was kept in an oven at 60ºC for 1 h. Then, substrate immersed in 20 g/l ethanol solution of lauric acid for 24 hours and dried in air for 24 hours. They reported the water contact angle of 163º and 173º and the sliding angle of 4º.

3.2 Physical Texturing:

Micro/nano's roughened structured surfaces involved several fabrication methods such as lithography, etching, deformation, deposition & transfer which is used to create roughness on the surface of the substrate[59]. A few physical texturing techniques implemented by researchers to obtain good superhydrophobic characteristics have been brief with major emphasis on plasma and ion beam techniques in this article by displaying their results.

Anodic oxidation has been reported by Jessensky et al.[60] in which the anodic oxidation of aluminium took place in the electrolyte solution. This process prevents the further oxidation of the aluminium and made it scratch resistant. High order of nano-structured reported through the anodizing process. Different Super-hydrophobic films prepared to have different surface roughness reported by Miwa et al.[61] and the calculation of sliding angle, contact angle investigated by developing a relationship between them and concluded that with the increase of contact angle of water droplet sliding angle decreases.

The standard photolithographic technique is reported by Sommers et al.[62] which is used to develop micro patterns on aluminium surfaces and came up with the increased value of contact angle. Further, they proposed the applications of micropatterned aluminium surfaces on air cooling applications. A novel technique reported by Dietz et al.[63] to develop superhydrophobic copper surface by exposing the copper to atmospheric conditions i.e. in the open air and then dissolve in acetic solution which oxidized it to CuO and reported the static contact angle ~ $153.1^{\circ} \pm 1.7^{\circ}$.

The different processes adopted by different researchers for superhydrophobic coating on metallic surfaces have been discussed with the material and methods they have used with their findings.

Mandal et al. [13] performed a micro-imprinting technique on aluminium (Al-1100) using steel mold to form micropillars of micro, nano, and hierarchical level. Further, they did the hotwire treatment followed by the calcination process for altering the wettability of the substrates. They have reported the static contact angle over 150° and its hysteresis is less than 5° especially for nano and hierarchical structures.

Bharathidasan et al. [14] prepared superhydrophobic steel tubes with a water contact angle of 165° and sliding angle of 3.12° by chemical spraying method which involves spray coating of

RTV11 silicon resin 3g, toluene 8ml, dibutyltin dilaurate (DBT) 4% magnetically stirred and coating on the substrate resulted in the formation of silicon pre-coated steel substrates. Then they prepared the hydrophobic PDMS film using 5ml PDMS, toluene 3ml, TEOS 1 ml, and 0.5 ml DBT, TEOS as crosslinker with the PDMS system. ZrO_2 particles dissolved in 15 ml toluene ultrasonically and then 5ml PDMS added. In this mixture 1ml of Tetraethylorthosilicate (TEOS) and 0.5 ml of DBT were added and stirred magnetically for 30 min and then sprayed on silicon pre-coated steel substrates. They also reported the improved thermal and better corrosion resistance of the coated substrates.

Li et al. [15] used aluminium as a substrate material, they performed the electrodeposition method for altering the morphology. First, they polished the aluminium surface with #1000 and #1200 sandpaper and ultrasonically cleaning performed in deionized water for 4-5 min. Further, it is immersed in a solution of 60 g/L NaOH aqueous solution and 10 vol% H_3PO_4 aqueous solutions for 10 min and cleaning with deionized water. Electrochemical etching is performed by making Cu plate as the cathode and Al plate as the anode in the electrolyte of 0.2 mol/L NaCl aqueous solution with a current density of 0.5 A/cm^2. The Ni-SiO2 composite coating on pre-treated Al alloy by making Ni plate as anode and Al alloy as cathode and solution of $NiSO_4•6H_2O$, $NiCl_2•6H_2O$, H_3BO_3, $C_{12}H_{25}SO_4Na$, $C_7H_5O_3NS$, $C_4H_6O_2$, and SiO_2 dissolved in deionized water. They reported a contact angle of 169.3° and sliding angle of 5.3° and improved corrosion-resistant Ni-SiO_2 coatings.

Rius-Ayra et al. [16] used an electrochemical deposition technique on aluminium substrate and reported the water contact angle of 170º ± 0.54º and sliding angle of 1º. The first ground the substrate using P1200 SiC abrasive paper and cleaning with ethanol. Then, a solution of 0.1 M lauric acid, 0.05 M ZnCl2, and 1 g/L of α-Al2O3 in ethanol is prepared and further aluminium substrates (anode and cathode) immersed in a solution with 2 cm distance between them with the current density of 0.02 A/dm^2 applied from 60 s to 1200 s, cleaned with ethanol and dried in the fume hood.

Gateman et al. [18] prepared the four different substrates of stainless steel 444 with a water contact angle of 145° ± 4 and 136° ± 4, 153° ± 1 and 157° ± 1. They used the thermal spray technique to obtain these results. They first sprayed the SS 444 plates using alumina grit blasting (270µm) to avoid the corrosion between the coating and substrate. Then to decrease the atomic particle size the SS powder was processed through high-energy ball milling. High voltage oxygen fuel spray gun is used to spray the coating of approx. 500µm thickness keeping parameters powder feed rate of 44 g/min, stand-off distance of 13", transversal speed of 0.5 m/s with a pitch step size of 10 mm, and 15 passes were performed. Four different samples were prepared by varying the velocity (500 to 800 m/s) and temperature conditions(1600-2100ºC).

Liu et al. [64] performed a spray coating technique on magnesium and aluminium alloys by preparing lanthanum hydroxide sol. Lanthanum hydroxide sol is sprayed onto the substrates to create a micro-nano fiber-like structure then the substrates were dissolved in the ethanol and stearic acid solution and make dry for 2 h at 120ºC. They reported the better corrosion resistance with high chemical and mechanical stability of the coated substrates with a water contact angle of 157° for both.

Yang et al. [65] used an electroplating chemical technique on aluminium in which they first prepared the electroplating solution by mixing 25 mL $CuSO_4$ aqueous solution and isometric ethylenediamine tetraacetic acid (EDTA), the ratio of concentration maintained as 1:1. Then, 0.3 mL formaldehyde was added to the solution, and its pH was adjusted between 11.5-12.5 by using 1 mol/NaOH aqueous solution. The substrate is cleaned in butyl acetate and rinsed in deionized water and dried. Copper coated aluminium substrate obtained by immersing in electroplating solution at room temperature further substrate treated with 5 mmol/L octadecanethiol ethanol solution for 30 min, then rinsed with ethanol 3 times and air-dried. They reported the water contact angle (WCA) of 153.6º.

4. Plasma process for Super-hydrophobic surfaces:

A Plasma is an ionized gas that is also considered as the fourth state of matter constituting 99% of the universe. Plasma is electrically neutral, and it contains an equal number of positive ions and electrons. It has high electrical conductivity and has free charge carriers. Plasma can be artificially created by providing energy to the gas. This energy is generally provided with the help of an electric source in the form of direct current (D.C.), A.C., radiofrequency (R.F.), and microwave frequency[66].

4.1 Creation of Plasma:

Plasma is created by applying a high voltage to the gas in the chamber at low pressure. Generally, the pressure maintained inside the chamber in the range of 10^{-3} torr to 10^{-1} torr. The schematic representation of a typical plasma set-up with the essential components required for the creation of plasma is shown in Fig: 8. These collisions further produce ions and electrons which further move towards the cathode and anode. Positive ions accelerate towards the cathode which results in the formation of Glow discharge. An electrical glow discharge is a type of luminous plasma created bypassing the voltage in the range of 100 V to several kV through a plasma gas (generally Argon Ar), this glow is produced as the number of collisions increased by excited electrons which generate photons between anode and cathode[67]. In this technique, the substrate on which coating needs to be done is attached to the anode and the coating material which is termed as the target material is attached with the cathode.

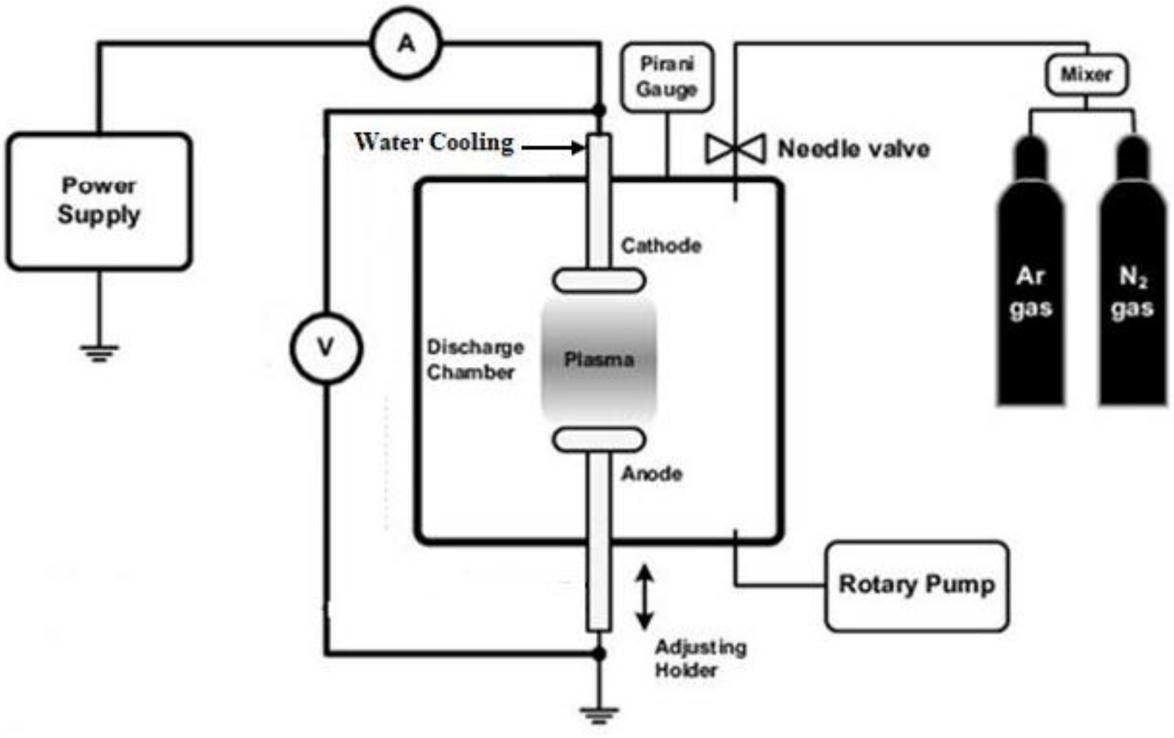

Figure 8: Schematic representation of a typical Plasma set-up with the essential components required for the creation of plasma (Figure Corrected)

Plasma technology has been widely used in every field varying from manufacturing to, automobile industry and for biomedical applications as well. In the medical field, plasma technology is used for the treatment of the wound, tumor, sterilization of surgical instruments[68].

Plasma technology has been widely used for treating the surface morphology through (i) plasma etching, (ii) plasma sputtering, and (iii) plasma polymerization. Plasma etching is generally used for increasing the surface roughness of the material, acting pre-treatment process for increasing the surface roughness on the material[69]. Plasma etching has also been used for generating micro-nano textured structures consisting of large bumps on the surfaces of the different materials, it is found to be an effective method for creating these hierarchical structures on the surface of a large number of materials in a single step[70]. Plasma etching has also been used for the creation of superhydrophobic surfaces and Anti-reflective surfaces by CF4 plasma, this technique reported optical reflectivity improved considerably and water contact angle is ~ 150º[71].

4.2 Sputtering:

Sputtering is a physical vapor deposition technique where the target material is bombarded with energetic ions and the sputtered atoms from the target material gets deposited onto the substrate surface as a coating film. It is the process of removal of atoms from the surface of the material under the impingement is known as sputtering. This technique was discovered in 1852 and further used by Langmuir for thin film deposition in the 1920s. The schematic diagram of the sputtering phenomenon is shown in fig:9

Plasma technology can be categorized depending upon their input power source for the generation of plasma i.e.

- DC (Direct Current) Plasma Sputtering
- DC Magnetron
- RF (Radiofrequency) Plasma Sputtering
- RF Magnetron
- Microwave Plasma Discharge

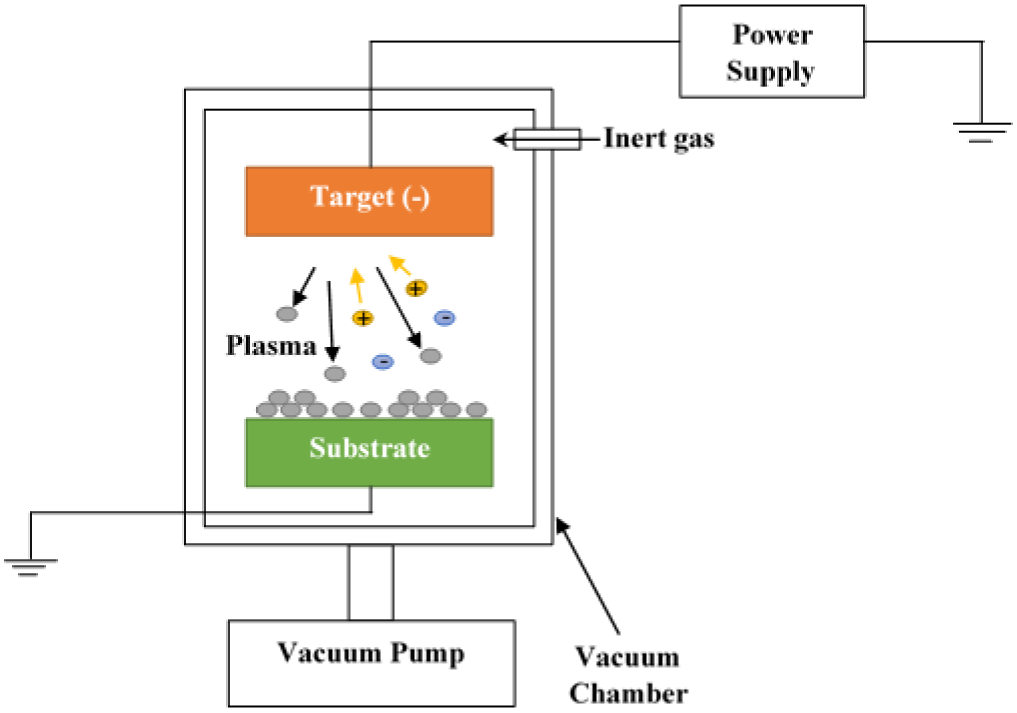

Figure 9: Representation of Sputtering using plasma and deposition of films

4.3 DC Plasma Sputtering:

DC power supply is connected across the two electrodes i.e. cathode and anode for generating plasma inside the chamber having suitable gas at low pressure. DC Plasma setup consists of the components like cathode (target material), gas injection system, anode on which substrate is kept, and vacuum pumping system which is responsible for maintaining the desired vacuum inside the chamber. In this technique commonly argon (Ar) ions used for bombarding the target material, these Ar atoms are injected into the vacuum chamber at a low pressure ranging from 1-10 mtorr, and 0.5-5 kV DC supply is used for ionizing the Argon atoms[72]. DC Plasma can be used for surface modification of the metals, fabrics by making the surfaces hydrophobic and superhydrophobic without using any chemical solvents which are harmful to our environmental conditions. Anupriyanka et al.[7] performed the DC Plasma technique by using O_2 as working gas and modified the PET (Polyethylene Terephthalate) fabric as superhydrophobic and superoleophobic for oil and water separation and reported the contact angle for water with the surface is 163°.

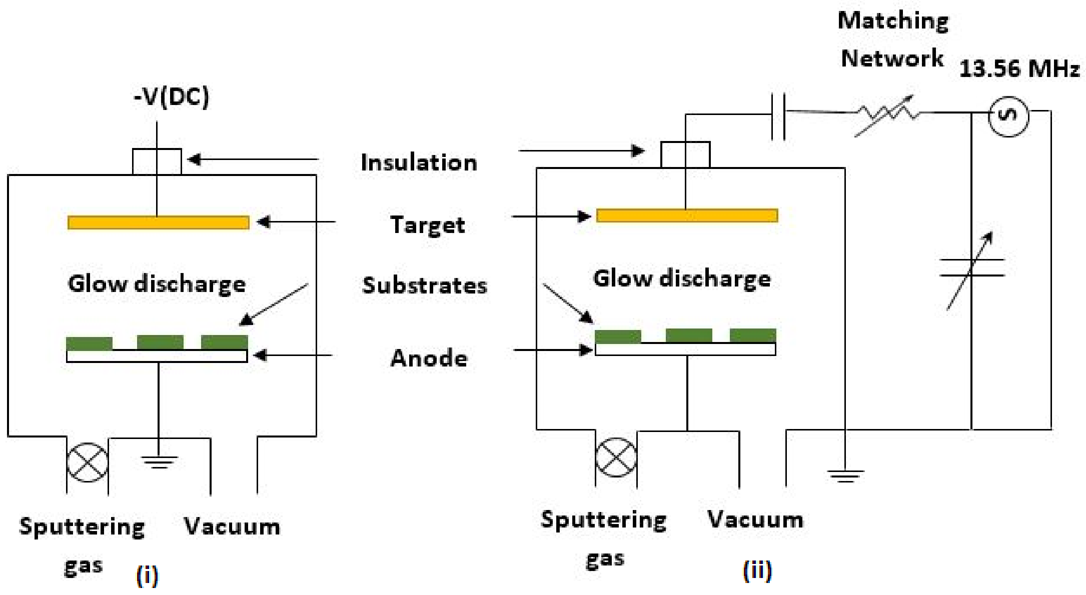

Figure 10: Schematic Representation of (i) DC Sputtering and, (ii) RF Sputtering technique

DC plasma sputtering is only used for the coating of conducting metals since insulating materials cannot be used as target material for deposition using this technique as space charge is created therefore ions will not go towards the cathode and the non-conducting coating prevents further flow of the electrons towards the anode [72] and the low deposition rate is also considered as another limitation of this technique. Therefore, to overcome the problems associated with DC Plasma sputtering technique like increasing the deposition rate DC Magnetron sputtering technique can be used and for solving the problem of charge accumulating on the coating material and for depositing the coating of insulating (Change) material RF technique can be used[73]. The basic difference between DC Sputtering and RF sputtering can be very well understood from the figure:10 i.e. DC sputtering required DC supply and RF sputtering required RF supply of 13.56 MHz and a matching network which is discussed later in detail. To obtain the high intensity of plasma and to increase the deposition rate DC Magnetron sputtering is used.

4.4 DC Magnetron Sputtering:

In this method, high intensity of plasma generated from which ions further extracted to bombard the target surface[74] due to the presence of Lorentz force which acts on the moving charged particle in a magnetic field and it is always acting at right angles to the direction of the motion of electron as per Fleming’s right-hand rule, therefore, the path of the electron will be circular as shown in fig:11. This technique has various advantages like high depositing rates, high purity of films, the heat-sensitive substrate can be coated easily, excellent uniformity can be obtained on the substrate having a large area[75]. The DC magnetron sputtering did not damage the material surface which is to be coated and provide less heating to it[72].

$$F = eV \times B = \frac{mv^2}{r} \tag{6}$$

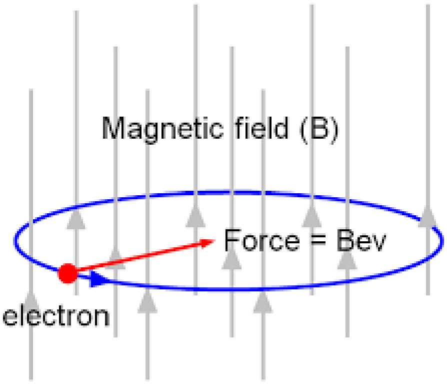

Figure 11: Force acting on moving electron in a magnetic field.

4.5 RF (Radiofrequency) Plasma Sputtering:

RF Plasma sputtering technique is useful for the coating of insulating materials onto the substrate at low pressure (~10^{-3} torr). It overcomes the limitation of DC sputtering as a coating of a non-conductive target is possible on to the substrate by using the RF power source of 13.56 MHz[76]. The schematic diagram for RF Plasma sputtering as shown in fig:10. Generally, a power supply of 13.56 MHz with 1~3 kW power with cathode using a matching network and blocking capacitor[77].The blocking capacitor acting as a conductor for RF as well as an isolator for DC-self bias negative potential[78].

The target potential changes during each half-cycle, in one-half cycle it becomes positive so that the electrons will flow towards the electrode and when it is negative the Ar ions move towards it therefore it acts as a cathode during some time in every cycle whereas in rest of the duration it will act as an anode. RF plasma sputtering offers few advantages i.e. easy to work with insulating targets, arcing is reduced, uniform coating deposition on the substrate[79]. A schematic diagram of RF Plasma sputtering is shown in fig: 12. To increase the intensity of plasma we will use the RF Magnetron plasma technique which increases the rate of deposition which is discussed next in this article.

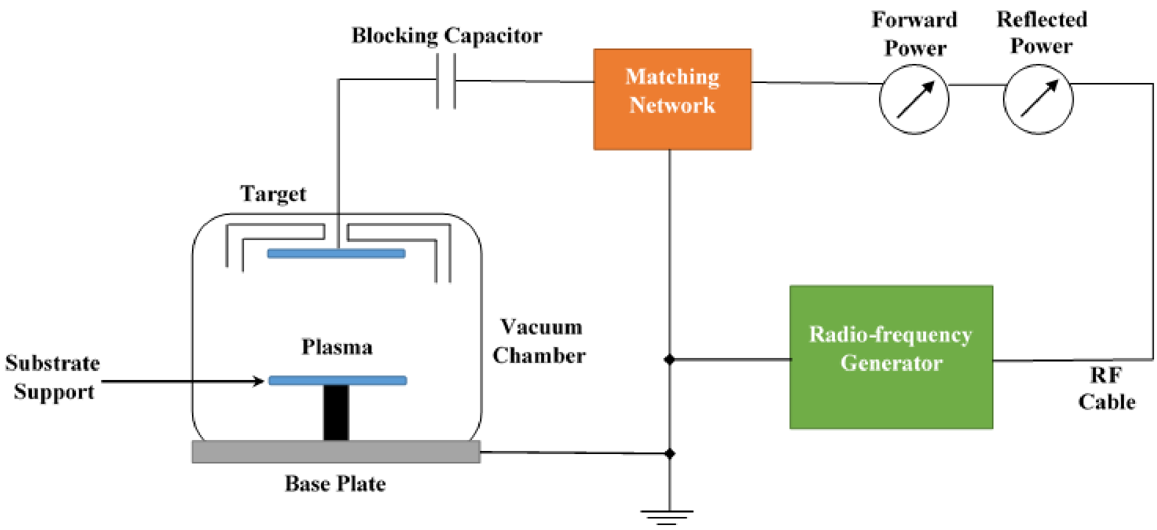

Figure 12: Schematic Diagram of RF Plasma Sputtering

4.6 RF Magnetron Sputtering:

Magnetron-based sputtering uses strong magnets attached near the target material surface which confine the path of the electrons resulting in a higher density of the plasma and higher deposition rate at the substrate surface[80]. This technique confines the plasma around the target material thereby develop a uniform thin film coating on to the substrate without degrading the quality of films, it overall improves the efficiency of the sputtering process and offers a vital number of additional advantages like depositing thin films of insulating materials, arching is reduced due to the use of RF field[81].

RF magnetron sputtering technique is the flexible technique that allows controlling the properties of the target electrode by providing uniform coating. This technique allows to control coating composition by varying the parameters like gas pressure, biasing of the substrate, and controlling the temperature during deposition, and it provides the flexibility of processing the plasma technique for complex structure[82]. The schematic view of RF Magnetron sputtering is very well understood from fig:13. An “electron trap” is created due to the intersection of the magnetic and electric field as the magnetic field holds the electron close to the target material due to which more collisions occur with the atoms of working gas[82].

RF magnetron sputtering used for generating super-hydrophobic coating on the substrate as reported in the literature i.e. this technique has been used for depositing silver and copper on metal sputtered super-hydrophobic surfaces by using Poly (Methyl Methacrylate) (PMMA) as the substrate[83]. They have used both silver and copper as a coating agent for fighting against the bacteria using an RF magnetron sputter reactor with Ar as the inert gas.

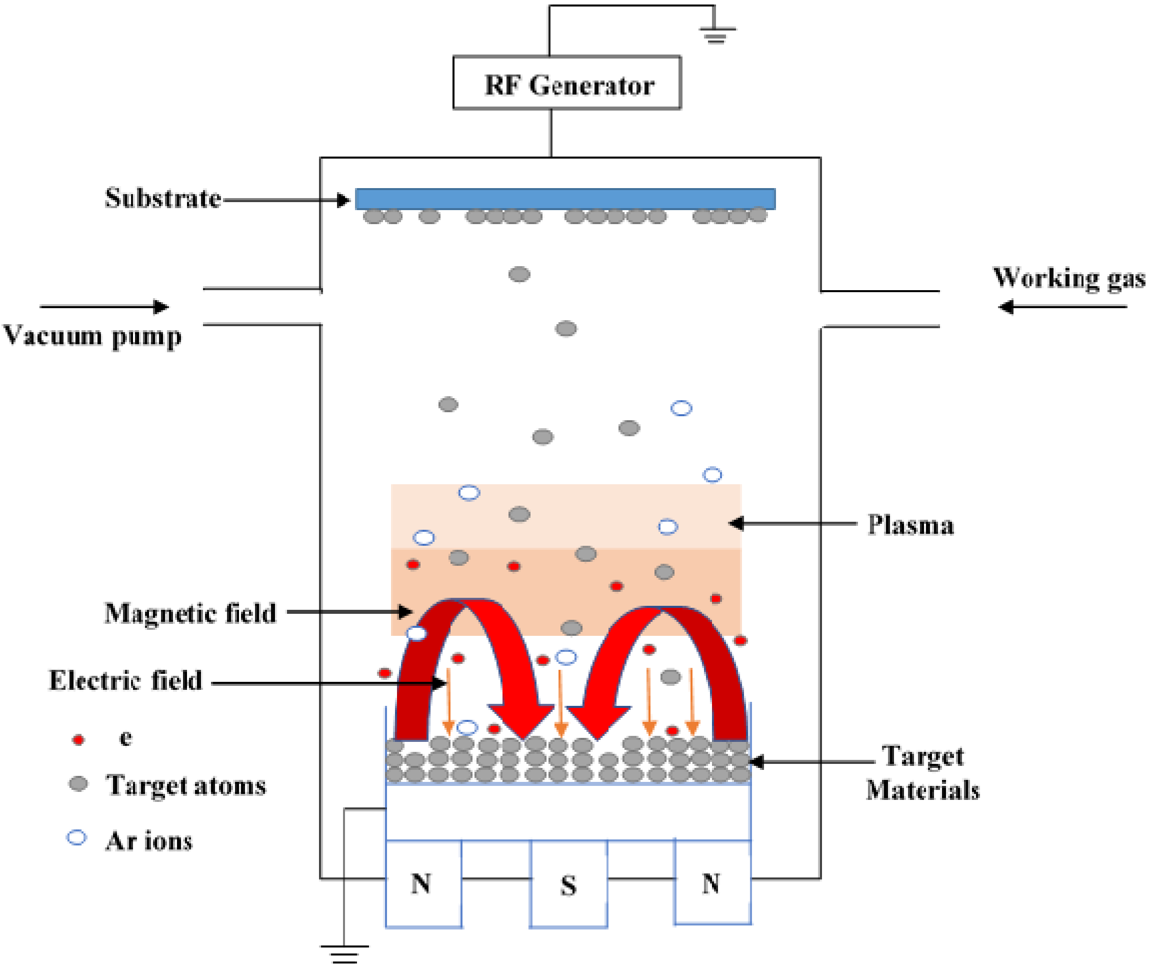

Figure 13: Schematic of RF Magnetron Sputtering

4.7 AC Plasma Sputtering:

AC sputtering technique uses AC (alternating) voltage to supply the power between the target material and the substrate. This process is generally used for the coating of non-conducting material onto the substrate with the frequency of 10-100 kHz[72]. AC discharge and DC discharge both have been investigated by Demina et al.[84] by doing plasma treatment on polyethylene terephthalate films and characterizes the surface structure and reported that the contact angle changes rapidly in case of AC discharge and led to the increase in more hydrophilic character.

4.8 Chemical Vapor Deposition (CVD) and plasma-enhanced CVD (PE-CVD):

The chemical vapor deposition (CVD) technique has been widely used for thin-film coating of metallic compounds, alloys, amorphous and crystalline materials on the substrate for changing their surface chemistry and morphology. CVD processes include the chemical reaction due to the use of several reactants and precursors which are essential for depositing the thin film. Several CVD processes can be classified i.e. Metal-organic CVD (MOCVD) in which metal-organic like trimethylaluminum can be used as a precursor, plasma-enhanced CVD (PECVD) where plasma used to alter the chemical reactions, low-pressure CVD (LPCVD) where the pressure of operating gas is low it can be in the range of 0.6-1.33 mbar, laser-assisted CVD which uses a laser to enhance chemical reactions and another one is Aerosol assisted CVD (AACVD) where liquid precursor used in the form of aerosol in the reactor due to which evaporation becomes easy[85].

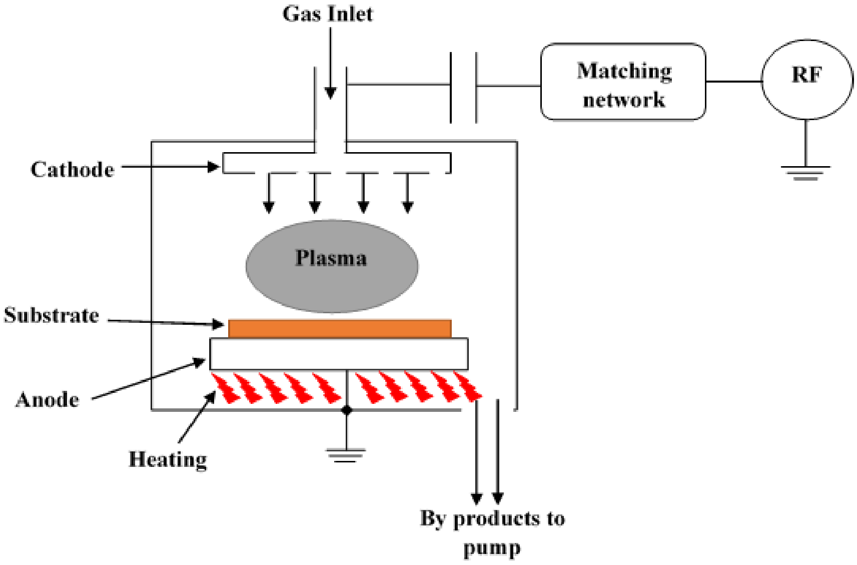

Figure 14: Schematic representation of PE-CVD reactor.

In the comparison of traditional CVD technique which requires high-temperature plasma-enhanced CVD (PECVD) technique is preferred as it operates at low temperature since plasma is being created between the two electrodes and space between them is filled with reactive gases. The schematic diagram of PE-CVD is shown in fig:14. The chemical reactions involved in CVD processes are decomposition, reduction, chemical transport reactions, and polymerization[77]. This technique is also used by the researcher for enhancing the heat transfer characteristics as reported by Safonov et al.[86] that heat transfer characteristics increased by 30% by depositing the fluoropolymer coatings on the stainless steel heater tubes by hot wire chemical vapor deposition (HWCVD) and also the nucleation site density increased by 5 times and the wetting contact angle reported to be 125° ± 2°.

4.9 Laser Texturing:

The femtosecond (fs) laser process has been widely used for altering the surface morphology in electrical, mechanical, and biomedical industrial applications in which the surface of the material is modified by using a femtosecond laser. It is a completely new technique for the fabrication of micro/nanotextured surfaces in a single step. As compared to other techniques laser micro-machining offers several advantages over other methods i.e. simple construction, efficient one-step process, the machining process is done through the beam of light, and contactless operation with the substrate material, applicable for any type of 3-D object[8].

Developing super-hydrophobic surfaces using the femtosecond laser process is quite simple and it is a fast process as compared to the conventional techniques used for preparing super-hydrophobic surfaces. Kietzig et al.[87] performed the laser processing using the polarized beam of Ti: Sapphire laser on very pure metals (Cu, Ti, Al, Co & Fe) with a repetition rate of 1 kHz and pulse duration of 150 fs reported the contact angle of about 160^o and very low contact angle hysteresis by exposing them to ambient air after laser treatment.

Further, multi-functional metal surfaces are processed using a femtosecond laser to produce hierarchical micro/nanostructures by using 65-fs pulses of Ti: Sapphire laser with a wavelength of 800 nm reported the increase of water repellence characteristics and self-cleaning on the samples of titanium, platinum, and brass and reported the water contact angle of 158^o and sliding angle of 4^o on a platinum surface with a fluence rate of 9.8 J/cm^2[88].

4.10 Ion-beam processing:

Ion beam machining has been widely used for the modification of integrated circuits and microelectronics applications. It can be categorized into two parts i.e. ion beam sputtering and deposition. Ion beam sputtering uses an ion source directly on the target, which is to be sputtered, an ion source in this sputtering technique consists of both cathode and anode and an electrostatic field is generated in the ion source by applying a high voltage field of 2-10 kV[89]. A working gas (Argon Ar) can be used for generating plasma which is injected through ion gun and because the high electric field is applied around the ion source it ionized the gas resulted in the formation of plasma thereby the ions are further moved from anode to cathode in the form of ion beam and then sputters the target to the substrate by the momentum transfer between ions and the target material[89]. Focussed ion beam sputtering technique is an emerging technique for industrial applications like fabrication of micro-milling tool, nanopillars, nanopores, AFM tip[90]. This technique can also be used for enhancing the surface hydrophobicity by increasing the surface roughness in a single step as performed by Park et al.[91] in which they fabricated the super-hydrophobic surface on Perfluoroalkoxy (PFA) films of 80 mm x 80 mm irradiated by 100 keV Xe^+ ions by varying the fluences ranging from 4 x 10^{16} to 7 x 10^{16} ions cm^{-2} and reported the contact angle of 150° by maintaining the pressure of 10^{-5} to 10^{-6} torr inside the target chamber and current density of ion beam is 30 µA cm^{-2}. Atom beam sputtering is another technique used for depositing the thin films on the substrate as performed by Singh et al.[92], they deposited the Ag films on a glass substrate and obtained a plasmonic surface with a fluence range of 1 x 10^{16} to 3 x 10^{16} ions/cm^2 through 1.5 keV Ar ion irradiation and reported that the contact angle increases by increasing fluence rate.

Atmospheric Plasma:

Atmospheric Pressure Plasma Jets were reported to be advantageous for medical applications. There are associated risk factors in using the plasma for the therapeutic purpose[93]. The Atmospheric plasma is created by supplying electrical energy, this energy is further transferred to the neutral species using collisions.

Plasma technology is also used for treating the surface of the polymers by the application of plasma gases like N_2, O_2, and NH_3, etc.[94]. It is also used in the electronic industry for several applications, like treating the semiconductors materials and processing them[95]. Plasma can be distinguished based on different gas pressure which categorized it into two different plasmas i.e., LTE (Local thermodynamic equilibrium) plasma and non-LTE (Non-local thermodynamic equilibrium) which changes the plasma nature[66]. Low pressure-based plasma technology has a variety of applications in our daily needs as well like the use of neon lamps and plasma T.V. set[96] and it is being used for thin-film metallic-based coatings on the surfaces. Low-pressure plasma technology has a technical limitation associated with it because of vacuum equipment[96]. Therefore, Atmospheric pressure plasma technology is being widely used for several industrial uses and surface treatment purposes.

5. Engineering the wettability by Plasma processing:

The author Fernandes et al.[8] took the Aluminium (Alclad AA2024-T3) alloy as the substrate and coating of HMDSO (hexamethyldisiloxane) monomer performed using capacitively coupled RF plasma reactor. They experimented with it in two stages, i.e. pre-treatment and deposition. In the first part, Aluminium is cleaned in Ar/H_2 plasma for 5 to 15 minutes at 80 mtorr discharge pressure and a -700 V self-bias on the powdered electrode with RF power of 185 W. Then, the deposition of HMDSO done using the gas mixture of (O_2, N_2, and H_2 at 30 sccm) at RF power of 11 W with a self-bias voltage of -190 V to -150 V, and the pressure in the chamber maintained to 30 mtorr until the coating thickness of 200 nm HMDSO is obtained. Fernandes et al. reported the improved corrosion-resistant behavior and good adhesive performance of plasma coated Aluminium. They have not reported the static contact angle and contact angle hysteresis.

Sahoo et al.[97] performed the composite hydrophobic coating on stainless steel plates using thermal plasma evaporation method in 50 KW plasma reactor, Argon (Ar) as working gas by keeping the flow rate of 1 L/min and reported the static contact angle 129.8°, 150.8°, and 146.3° by varying the deposition time as 1 min, 2 min and 3 minutes respectively.

Nokes et al.[98] performed the Ar Plasma treatment on the Polyolefin film clamped between the two glass slides with 60 W power and 200 mtorr gas pressure and measured the contact angle and contact angle hysteresis greater than 150º, by varying the Ar plasma exposure time of 30 min or higher (154° ± 6° for 30 min, 158° ± 4° for 40 min, and 158° ± 3° for 60 min). Kefallinou et al.[83] developed metal (Cu and Ag) sputtered super-hydrophobic surface for antibacterial action by using RF Magnetron sputtering technique with Ar as the inert gas with Ar pressure of 3 mtorr. They have used copper and silver coating deposited on PMMA Poly (Methyl Methacrylate) by maintaining the base pressure of 5×10^{-8} torr in a plasma reactor and reported the contact angle of 158 ± 2º.

Ko et al.[99] used the O_2 plasma etching on the surface of Polyethylene terephthalate (PET) as a substrate by placing the metallic mesh of stainless steel for developing nanostructures using RF of 13.56 MHz, after O_2 plasma etching super-hydrophobic coating of HMDSO (Hexamethyldisiloxane) is deposited on PET substrate by plasma polymerization for 10 sec at -400 V, Vacuum chamber base pressure $\leq 1\ mTorr$, Operating pressure 20 mTorr, O_2 flow rate 20 sccm. They reported the contact angle of 164 ± 2.2º after the plasma treatment of 60 min.

Plasma treatment is not limited to developing the hydrophobic and super-hydrophobic surfaces but also used for making the surface hydrophilic as done by Demina et al.[84] in which they have performed both DC and AC plasma treatment on Poly (Ethylene terephthalate) (PET films), first AC plasma treatment is performed by maintaining base pressure of 20 mtorr operating at 40 kHz, working gas flow rate 20 sccm, glow discharge ignited at 50 W within 10-

60 s and then DC Plasma treatment (50 mA) with working gas pressure maintained is ~ 150 mtorr and then reported a drop in contact angle measurement from 80º to 17º in case of AC discharge and 10-12º in case of DC discharge.

Chauhan et al.[100] reported the static contact angle of 98.5º on silicon and corning glass by depositing zirconium films by RF Magnetron sputtering process by maintaining the distance between the substrate and target as 50 mm and argon Ar used as working gas with a flow rate of 4 sccm and 20 sccm with pressure maintained inside the vacuum chamber is 3.75 x 10^{-3} mtorr. Plasma technique has also been used for making superhydrophobic fabric surfaces mainly for oil and water separation as done by Anupriyanka et al.[7]. DC plasma technique is used for making Polyethylene Terephthalate (PET) fabric as superhydrophobic and reported the contact angle of 163º for water exhibiting super-hydrophobic surface and superoleophobic for ethylene glycol, the fabric was treated with O_2 DC plasma discharge keeping the base pressure as 37.5 mtorr, discharge potential 300 V and exposure time of 5 min.

Minarik et al.[101] reported the contact angle of 146º± 2º and 139º ± 1º by varying the plasma power from 300 W to 250 W respectively on Polystyrene (PS) Petri dishes by applying CF_4 plasma for nanostructure generation on polystyrene micro-structured surface. Plasma power of 1200 W with a frequency of 13.56 MHz with a gas pressure of 525 mtorr, before plasma treatment they modified the surfaces with spin coating and chemically a solvent mixture deposited on PS dishes with a specially constructed dosing device (time-sequenced phase separation chamber) rotating at 2200 rpm.

Ryu et al.[102] reported the rapid increase of the contact angle from 66º to 142º and improved the dropwise condensation by 205% on the aluminium (Al6061) substrate. They deposited the coating of F-DLC (Fluorine doped diamond-like carbon) by PECVD (Plasma enhanced chemical vapor deposition) technique using magnetron sputtering, with gaseous media C_2H_2 and a mixed gas of C_2H_2 and CF_4 injected into two linear ion sources in the ratio 1:3. The vacuum was maintained ∼10 Pa using rotary and mechanical booster pump and ∼ 10^{-3} Pa using turbo molecular pump. Before coating microblasting technique was used to fabricate microtextures on the surface of a substrate in a blasting system by spraying stainless steel powder (22 to 63 µm diameter) through the nozzle which produces etching. This technique is used to develop micro-texture on the surface of aluminium Al6061. The experimental setup consists of the components like a blasting chamber, dust collecting unit, air-controlling unit, dual-stage cyclone, heater, rotary table, and blasting sensors.

Subeshan et al.[103] treated the Aluminium 2024-T3 alloy with O_2 plasma treatment by varying radiofrequency levels from low to high. They reported the water contact angle of 168.54° and 167.34° and sliding angle as 5° by working with 8 minutes high-intensity RF and 8 minutes medium-intensity of RF plasma. Two thin layers of Xylene, t-butyl acetate, and Acetone were applied on the substrate as a bottom coating to eliminate the uncoated regions thereby dried for 2h at room temp. After that, the substrate is cleaned using oxygen plasma cleaner (Harrick Plasma Cleaner) by placing it in a vacuum maintaining the pressure level as -375.03 torr and then a top coating of Acetone with micro-nano scale particles applied using a spray gun and followed by heat treatment at 150°C for 1h.

Liu et al.[104] also reported the maximum value of the contact angle as 167.9° ± 1.8° by depositing boron nitride nanosheets (BNSS) on silicon substrate by chemical vapor deposition at 1000°C with the flow of NH_3 at a rate of 30 sccm for 30 min and then BNSS functionalization performed through low-pressure plasma treatment with RF power of 40 W with a gas mixture of Ar/SF_6 by maintaining the pressure range between 0.075 torr to 0.15 torr.

Orazbayev et al.[105] prepared the superhydrophobic surfaces using PECVD methods through RF plasma discharge at low pressure and plasma jet at atmospheric pressure on the glass and silicon substrates and reported the contact angle of 160° in Ar/CH_4 plasma through PECVD method which was varied to 135° in a time of 18 months and the contact angle of 135° varied to 120° in a period of 6 months using Ar/CH_4 plasma jet. The upper electrode is connected with RF power supply of 13.56 MHz, MFC Bronkhorst gas flow meter controlled the mixture of 50 sccm and 5 sccm (Ar and CH_4/C_2H_2), pressure fixed as 0.6 mbar, length of the quartz glass tube is 70 mm, outer diameter is 10 mm & inner diameter is 3 mm, copper used as grounding electrode and atmospheric discharge power of 0-50 W is maintained.

The findings of the different plasma-based techniques used for making the super-hydrophobic surfaces are listed in the Table:1 presented below:

S.No:	**Reference**	**Technique**	**Substrate Material**	**Coating Material**	**Main Findings**			**Other Findings**
					CA (θ) degrees	**Sliding angle(degrees)**	**CAH (degrees)**	
1.	Anupriyanka et al.[7]	DC Plasma	Polyethylene terephthalate (PET) fabric	O_2 plasma	163°	Not reported	Not reported	Superoleophilic for ethylene glycol

2.	Demina et al.[84]	AC and DC Plasma	Polyethylene terephthalate (PET)	Chitosan	17° 10-12°	Not reported	Not reported	-
3.	Fernandes et al.[8]	RF Plasma	Aluminium (Alclad AA2024-T3 alloy)	Hexamethyl disiloxane monomer (HMDSO)	Not reported	Not reported	Not reported	Improved Corrosion resistance & adhesive performance
4.	Ko et al.[99]	RF Plasma-based ion etching	Polyethylene terephthalate (PET)	HMDSO (Hexamethyldisiloxane)	164 ± 2.2°	Not reported	10° 2.7°	-
5.	Subeshan et al.[103]	RF Plasma	Aluminium 2024-T3	Acetone with micro/nanoparticles	168.5° 167.3°	5°	Not reported	-
6.	Kefallinou et al.[83]	RF Magnetron	Poly (Methyl Methacrylate) (PMMA)	Copper and Silver	158 ±2°	Not reported	2° 1°	Copper shows better Antibacterial properties
7.	Orazbayev et al.[105]	RF Plasma & Plasma Jet	Glass and Silicon	Ar/CH_4Plasma gas	160° 135°	Not reported	Not reported	-
8.	Chauhan et al.[100]	RF Magnetron	Silicon and corning glass	Zirconium	98.5°	Not reported	Not reported	-
9.	Minarik et al.[101]	Chemical method & RF Plasma	Polystyrene (PS) Petri Dishes	CF_4 plasma	146° 143° 139°	5°±1° 8°±1°	Not reported	-
10.	Liu et al.[104]	CVD& RF Plasma	Silicon (Si/SiO2)	Boron nitride nanosheets (BNNS)	137°±1.4° 167.9°±1.8°	Not reported	Not reported	-
11.	Nokes et al.[98]	Ar gas Plasma	Glass slide	Polyolefin films	154° 158°	Not reported	6° ± 1°	-
12.	Ryu et al.[102]	Microblasting& PECVD Magnetron	Aluminium Al6061	Fluorine-doped diamond-like carbon (F- DLC)	142°	41°	1°	Heat transfer efficiency increased by 205%

13.	Jafari et al.[106]	Atmospheric pressure Plasma Jet	Aluminium 6061	HMDSO (Hexamethyldisiloxane)	163º	1º	Not reported	-
14.	Siddaramanna et al.[107]	Chemical Method	Aluminium (AA-6061-T6)	[SA]/[Zn2+]	165 ± 2°	Not reported	4º	-
15.	Safonov et al.[86]	CVD	Stainless steel tubes (AISI 321)	Fluoropolymer	125º±2º	Not reported	Not reported	30% heat transfer increases. Nucleation site density increases. Bubble departure diameter increases.
16.	Sahoo et al.[97]	Thermal Plasma	316L stainless steel	Polycarbosilane	129.8°150.8° 146.3°	7º 5º 2º	Not reported	-
17.	Sharifi et al.[108]	Plasma Spraying	Stainless steel	TiO_2	150º 156º 167º	Less than 10º	Not reported	-
18.	Sharifi et al.[109]	Plasma Spraying	304 Stainless Steel	TiO_2powder	165º	1.5º	Not reported	-
19.	Huang et al.[110]	Plasma Spraying CVD	Stainless Steel	Al & WO_3powder	157 ±1°	7.5 ± 1°	Not reported	-
20.	Sarbada et al.[111]	Laser	Copper and PDMS	Ti-Sapphire femtosecond laser	165º 153º	Not reported	Not reported	-
21.	Li et al.[9]	Laser & Ion Implantation	Copper	Carbon	152.1° ±1°	Not reported	Not reported	-
22.	Li et al.[112]	Laser	Titanium Alloy Ti6A4V	Nanosecond pulsed laser	153º	Not reported	Not reported	Light absorbing capacity improved

7. Summary and Conclusion:

Superhydrophobic surfaces have tremendous applications due to their surface ability to repel the liquid droplets and acting as a self-cleaning surface which makes them more durable for their industrial use. The superhydrophobic metallic surfaces being corrosive resistant can have a lot of impact in the future which motivates the researchers to build superhydrophobic metallic coated material. Several techniques were used by the researchers for developing superhydrophobic coating. Plasma technique is an environmentally friendly, easy, and fast method to engineer the wettability of the superhydrophilic or superhydrophobic. These latest innovations in the technology in the field of surface coating motivate the researchers to bring a new revolution in developing the superhydrophobic metallic coating in the future.

References:

[1] Theory of Wetting Action at Solid Surfaces, n.d.

[2] B. Thomas Young, M.D. For Sec, III. An essay on the cohesion of fluids, Philosophical Transactions of the Royal Society of London. 95 (1805) 65–87. https://doi.org/10.1098/rstl.1805.0005.

[3] Drop Dynamics and Dropwise Condensation on Textured Surfaces | Sameer Khandekar | Springer, (n.d.). https://www.springer.com/gp/book/9783030484606 (accessed September 4, 2020).

[4] J. Jeevahan, M. Chandrasekaran, G. Britto Joseph, R.B. Durairaj, G. Mageshwaran, Superhydrophobic surfaces: a review on fundamentals, applications, and challenges, Journal of Coatings Technology and Research. 15 (2018) 231–250. https://doi.org/10.1007/s11998-017-0011-x.

[5] J.I. Lim, S. il Kim, Y. Jung, S.H. Kim, Fabrication and medical applications of lotus-leaf-like structured superhydrophobic surfaces, Polymer (Korea). 37 (2013) 411–419. https://doi.org/10.7317/pk.2013.37.4.411.

[6] M. Ferrari, A. Benedetti, Superhydrophobic surfaces for applications in seawater, Advances in Colloid and Interface Science. 222 (2015) 291–304. https://doi.org/10.1016/j.cis.2015.01.005.

[7] T. Anupriyanka, G. Shanmugavelayutham, B. Sarma, M. Mariammal, A single step approach of fabricating superhydrophobic PET fabric by using low pressure plasma for oil-water separation, Colloids and Surfaces A: Physicochemical and Engineering Aspects. 600 (2020). https://doi.org/10.1016/j.colsurfa.2020.124949.

[8] J.C.S. Fernandes, M.G.S. Ferreira, D.B. Haddow, A. Goruppa, R. Short, D.G. Dixon, Plasma-polymerised coatings used as pre-treatment for aluminium alloys, 2002.

[9] Y. Li, M. Li, Y. Utaka, C. Yang, M. Wang, Effect of copper surface modification applied by combined modification of metal vapor vacuum arc ion implantation and laser texturing on anti-frosting property, Energy and Buildings. 223 (2020) 110132. https://doi.org/10.1016/j.enbuild.2020.110132.

[10] M. Khodaei, Introductory Chapter: Superhydrophobic Surfaces - Introduction and Applications, in: Superhydrophobic Surfaces - Fabrications to Practical Applications, IntechOpen, 2020. https://doi.org/10.5772/intechopen.85359.

[11] Y.C. Jung, B. Bhushan, Wetting behaviour during evaporation and condensation of water microdroplets on superhydrophobic patterned surfaces, 2008. https://doi.org/https://doi.org/10.1111/j.1365-2818.2007.01875.x.

[12] B. Singh Sikarwar, S. Khandekar, K. Muralidhar, EFFECT OF SURFACE HYDROPHOBICITY ON HEAT TRANSFER DURING DROPWISE CONDENSATION: A NUMERICAL STUDY, n.d.

[13] P. Mandal, J. Ivvala, H.S. Arora, H.S. Grewal, Sustainable approach for the development of durable superhydrophobic metallic surfaces, Materials Letters. 279 (2020). https://doi.org/10.1016/j.matlet.2020.128516.

[14] T. Bharathidasan, S. Sathiyanaryanan, Self- replenishing superhydrophobic durable polymeric nanocomposite coatings for heat exchanger channels in thermal management applications, Progress in Organic Coatings. 148 (2020). https://doi.org/10.1016/j.porgcoat.2020.105828.

[15] X. Li, S. Yin, H. Luo, Fabrication of robust superhydrophobic Ni–SiO2 composite coatings on aluminum alloy surfaces, Vacuum. 181 (2020). https://doi.org/10.1016/j.vacuum.2020.109674.

[16] O. Rius-Ayra, N. LLorca-Isern, Growth of a superhydrophobic coating on an aluminium substrate with strong adhesive properties and showing efficient oil/water separation, Thin Solid Films. 710 (2020). https://doi.org/10.1016/j.tsf.2020.138259.

[17] H. Wang, G. Chi, Y. Wang, F. Yu, Z. Wang, Fabrication of superhydrophobic metallic surface on the electrical discharge machining basement, Applied Surface Science. 478 (2019) 110–118. https://doi.org/10.1016/j.apsusc.2019.01.102.

[18] S.M. Gateman, K. Page, I. Halimi, A.R.C. Nascimento, S. Savoie, R. Schulz, C. Moreau, I.P. Parkin, J. Mauzeroll, Corrosion of One-Step Superhydrophobic Stainless-Steel Thermal Spray Coatings, ACS Applied Materials and Interfaces. 12 (2020) 1523–1532. https://doi.org/10.1021/acsami.9b17836.

[19] W. Xu, C.H. Choi, From sticky to slippery droplets: Dynamics of contact line depinning on superhydrophobic surfaces, Physical Review Letters. 109 (2012) 024504. https://doi.org/10.1103/PhysRevLett.109.024504.

[20] B. Bhushan, Y.C. Jung, K. Koch, Micro-, nano- and hierarchical structures for superhydrophobicity, self-cleaning and low adhesion, Philosophical Transactions of the Royal Society A: Mathematical, Physical and Engineering Sciences. 367 (2009) 1631–1672. https://doi.org/10.1098/rsta.2009.0014.

[21] B. Bhushan, Y.C. Jung, Wetting, adhesion and friction of superhydrophobic and hydrophilic leaves and fabricated micro/nanopatterned surfaces, Journal of Physics Condensed Matter. 20 (2008). https://doi.org/10.1088/0953-8984/20/22/225010.

[22] P.G. de Gennes, Wetting: statics and dynamics, 1985.

[23] L. Legert, J.F. Joannys, Liquid spreading, 1992. http://iopscience.iop.org/0034-4885/55/4/001.

[24] wenzel1949, (n.d.).

[25] C. Neinhuis, W. Barthlott, Characterization and Distribution of Water-repellent, Self-cleaning Plant Surfaces, 1997.

[26] Lotus Effect, (n.d.). http://ice.chem.wisc.edu/Oil/On_The_Surface,_Its_All_About_Nano/Lotus_Effect.html (accessed July 15, 2020).

[27] The lotus leaf: how nature makes water-repellent materials., (n.d.). https://www.jeremyjordan.me/lotus-leaf-how-nature-makes-water-repellant-materials/ (accessed July 15, 2020).

[28] R.S. Hebbar, A.M. Isloor, A.F. Ismail, Contact Angle Measurements, in: Membrane Characterization, Elsevier Inc., 2017: pp. 219–255. https://doi.org/10.1016/B978-0-444-63776-5.00012-7.

[29] N. Nuraje, W.S. Khan, Y. Lei, M. Ceylan, R. Asmatulu, Superhydrophobic electrospun nanofibers, Journal of Materials Chemistry A. 1 (2013) 1929–1946. https://doi.org/10.1039/c2ta00189f.

[30] H.B. Eral, D.J.C.M. 'T Mannetje, J.M. Oh, Contact angle hysteresis: A review of fundamentals and applications, Colloid and Polymer Science. 291 (2013) 247–260. https://doi.org/10.1007/s00396-012-2796-6.

[31] E.J. de Souza, L. Gao, T.J. McCarthy, E. Arzt, A.J. Crosby, Effect of contact angle hysteresis on the measurement of capillary forces, Langmuir. 24 (2008) 1391–1396. https://doi.org/10.1021/la702188t.

[32] B. He, J. Lee, N.A. Patankar, Contact angle hysteresis on rough hydrophobic surfaces, Colloids and Surfaces A: Physicochemical and Engineering Aspects. 248 (2004) 101–104. https://doi.org/10.1016/j.colsurfa.2004.09.006.

[33] johnson1964, (n.d.).

[34] D.C. Pease, The significance of the contact angle in relation to the solid surface, Journal of Physical Chemistry. 49 (1945) 107–110. https://doi.org/10.1021/j150440a007.

[35] B. Singh Sikarwar, MODELING DROPWISE CONDENSATION UNDERNEATH INCLINED TEXTURED SURFACES, 2012.

[36] L.C.F. Blackman, M.J.S. Dewar, H. Hampson, An investigation of compounds promoting the dropwise condensation of steam, Journal of Applied Chemistry. 7 (2007) 160–171. https://doi.org/10.1002/jctb.5010070403.

[37] R.C.H. Watson, D.C.P. Birt, C.W. Honour, B.W. Ash, The promotion of dropwise condensation by montan wax. I. Heat transfer measurements, Journal of Applied Chemistry. 12 (2007) 539–546. https://doi.org/10.1002/jctb.5010121204.

[38] X.H. Ma, B.X. Wang, D.Q. Xu, J.F. Lin, Lifetime test of dropwise condensation on polymer-coated surfaces, Heat Transfer - Asian Research. 28 (1999) 551–558. https://doi.org/10.1002/(sici)1523-1496(1999)28:7<551::aid-htj1>3.0.co;2-d.

[39] S. Vemuri, K.J. Kim, B.D. Wood, S. Govindaraju, T.W. Bell, Long term testing for dropwise condensation using self-assembled monolayer coatings of n-octadecyl mercaptan, Applied Thermal Engineering. 26 (2006) 421–429. https://doi.org/10.1016/j.applthermaleng.2005.05.022.

[40] Q. Zhao, D.C. Zhang, J.F. Lin, G.M. Wang, Dropwise condensation on L - B film surface, Chemical Engineering and Processing: Process Intensification. 35 (1996) 473–477. https://doi.org/10.1016/S0255-2701(96)04158-X.

[41] R. Erb, E.T.A.C. Society, undefined Detroit, undefined Michigan, undefined USA, undefined 1965, Dropwise condensation on hydrophobic metal and metal-sulfide surfaces, (n.d.).

[42] R. Erb, E. Thelen, Dropwise condensation characteristics of permanent hydrophobic systems, (1966).

[43] R. Erb, E. Thelen, PROMOTING PERMANENT DROPWISE CONDENSATION, Industrial & Engineering Chemistry. 57 (1965) 49–52. https://doi.org/10.1021/ie50670a009.

[44] X. Ma, J. Chen, D. Xu, J. Lin, C. Ren, Z. Long, Influence of processing conditions of polymer film on dropwise condensation heat transfer, International Journal of Heat and Mass Transfer. 45 (2002) 3405–3411. https://doi.org/10.1016/S0017-9310(02)00059-5.

[45] P.J. Marto, D.J. Looney, J.W. Rose, A.S. Wanniarachchi, Evaluation of organic coatings for the promotion of dropwise condensation of steam, International Journal of Heat and Mass Transfer. 29 (1986) 1109–1117. https://doi.org/10.1016/0017-9310(86)90142-0.

[46] G. Koch, D.C. Zhang, A. Leipertz, Condensation of steam on the surface of hard coated copper discs, Heat and Mass Transfer/Waerme- Und Stoffuebertragung. 32 (1997) 149–156. https://doi.org/10.1007/s002310050105.

[47] R.A. Erb, Dropwise Condensation on Gold IMPROVING HEAT TRANSFER IN STEAM CONDENSERS, n.d. https://link.springer.com/content/pdf/10.1007/BF03215172.pdf (accessed September 4, 2020).

[48] X.H. Ma, B.X. Wang, D.Q. Xu, J.F. Lin, Lifetime test of dropwise condensation on polymer-coated surfaces, Heat Transfer - Asian Research. 28 (1999) 551–558. https://doi.org/10.1002/(sici)1523-1496(1999)28:7<551::aid-htj1>3.0.co;2-d.

[49] Q. Zhao, B.M. Burnside, Dropwise condensation of steam on ion implanted condenser surfaces, Heat Recovery Systems and CHP. 14 (1994) 525–534. https://doi.org/10.1016/0890-4332(94)90055-8.

[50] Q. Zhao, D. Zhang, S. Li, D. Xu, G. Zhang, J.L.-Proc.Iv.W.Cong.Chem. Eng, undefined 1991, New surface materials with dropwise condensation, (n.d.).

[51] V. Baghel, B.S. Sikarwar, D.K. Sharma, D.K. Avasthi, A correlation of metallic surface roughness with its hydrophobicity for dropwise condensation, in: Materials Today: Proceedings, Elsevier Ltd, 2020: pp. 1446–1452. https://doi.org/10.1016/j.matpr.2019.10.034.

[52] B. Qian, Z. Shen, Fabrication of superhydrophobic surfaces by dislocation-selective chemical etching on aluminum, copper, and zinc substrates, Langmuir. 21 (2005) 9007–9009. https://doi.org/10.1021/la051308c.

[53] Y. Huang, D.K. Sarkar, X. Grant Chen, Superhydrophobic aluminum alloy surfaces prepared by chemical etching process and their corrosion resistance properties, Applied Surface Science. 356 (2015) 1012–1024. https://doi.org/10.1016/j.apsusc.2015.08.166.

[54] R. Liao, Z. Zuo, C. Guo, Y. Yuan, A. Zhuang, Fabrication of superhydrophobic surface on aluminum by continuous chemical etching and its anti-icing property, Applied Surface Science. 317 (2014) 701–709. https://doi.org/10.1016/j.apsusc.2014.08.187.

[55] T.A. Saleh, N. Baig, Efficient chemical etching procedure for the generation of superhydrophobic surfaces for separation of oil from water, Progress in Organic Coatings. 133 (2019) 27–32. https://doi.org/10.1016/j.porgcoat.2019.03.049.

[56] H.R. Talesh Bahrami, B. Ahmadi, H. Saffari, Preparing superhydrophobic copper surfaces with rose petal or lotus leaf property using a simple etching approach, Materials Research Express. 4 (2017). https://doi.org/10.1088/2053-1591/aa6c3b.

[57] C. Chen, S. Yang, L. Liu, H. Xie, H. Liu, L. Zhu, X. Xu, A green one-step fabrication of superhydrophobic metallic surfaces of aluminum and zinc, Journal of Alloys and Compounds. 711 (2017) 506–513. https://doi.org/10.1016/j.jallcom.2017.04.050.

[58] P. Varshney, S.S. Mohapatra, Durable and regenerable superhydrophobic coatings for brass surfaces with excellent self-cleaning and anti-fogging properties prepared by immersion technique, Tribology International. 123 (2018) 17–25. https://doi.org/10.1016/j.triboint.2018.02.036.

[59] B. Bhushan, Y.C. Jung, Natural and biomimetic artificial surfaces for superhydrophobicity, self-cleaning, low adhesion, and drag reduction, Progress in Materials Science. 56 (2011) 1–108. https://doi.org/10.1016/j.pmatsci.2010.04.003.

[60] O. Jessensky, F. Müller, U. Gösele, Self-organized formation of hexagonal pore arrays in anodic alumina, Applied Physics Letters. 72 (1998) 1173–1175. https://doi.org/10.1063/1.121004.

[61] M. Miwa, A. Nakajima, A. Fujishima, K. Hashimoto, T. Watanabe, Effects of the surface roughness on sliding angles of water droplets on superhydrophobic surfaces, Langmuir. 16 (2000) 5754–5760. https://doi.org/10.1021/la991660o.

[62] A.D. Sommers, A.M. Jacobi, Creating micro-scale surface topology to achieve anisotropic wettability on an aluminum surface, Journal of Micromechanics and Microengineering. 16 (2006) 1571–1578. https://doi.org/10.1088/0960-1317/16/8/018.

[63] C. Dietz, K. Rykaczewski, A.G. Fedorov, Y. Joshi, Visualization of droplet departure on a superhydrophobic surface and implications to heat transfer enhancement during dropwise condensation, Applied Physics Letters. 97 (2010) 033104. https://doi.org/10.1063/1.3460275.

[64] L. Liu, J. Lei, L. Li, J. Zhang, B. Shang, J. He, N. Li, F. Pan, Robust Rare-Earth-Containing Superhydrophobic Coatings for Strong Protection of Magnesium and Aluminum Alloys, Advanced Materials Interfaces. 5 (2018). https://doi.org/10.1002/admi.201800213.

[65] H. Yang, Y. He, Z. Wu, J. Miao, F. Yang, Z. Lu, Fabrication of a superhydrophobic and high-glossy copper coating on aluminum substrates, Applied Surface Science. 433 (2018) 1192–1196. https://doi.org/10.1016/j.apsusc.2017.10.130.

[66] A. Grill, Cold plasma in materials fabrication, 1994. https://ieeexplore.ieee.org/iel1/27/7381/x0168351.pdf (accessed July 16, 2020).

[67] Electric glow discharge | Plasma-Universe.com, (n.d.). https://www.plasma-universe.com/electric-glow-discharge/ (accessed September 5, 2020).

[68] K.D. Weltmann, E. Kinde, T. von Woedtke, M. Hähnel, M. Stieber, R. Brandenburg, Atmospheric-pressure plasma sources: Prospective tools for plasma medicine, in: Pure and Applied Chemistry, 2010: pp. 1223–1237. https://doi.org/10.1351/PAC-CON-09-10-35.

[69] R. Jafari, S. Asadollahi, M. Farzaneh, Applications of plasma technology in development of superhydrophobic surfaces, Plasma Chemistry and Plasma Processing. 33 (2013) 177–200. https://doi.org/10.1007/s11090-012-9413-9.

[70] R. di Mundo, M. Troia, F. Palumbo, M. Trotta, R. D'Agostino, Nano-texturing of transparent polymers with plasma etching: Tailoring topography for a low reflectivity, Plasma Processes and Polymers. 9 (2012) 947–954. https://doi.org/10.1002/ppap.201200041.

[71] W. Somrang, S. Denchitcharoen, P. Eiamchai, M. Horprathum, C. Chananonnawathorn, Superhydrophobic and antireflective surface of nanostructures fabricated by CF 4 plasma etching, 2018. www.sciencedirect.comwww.materialstoday.com/proceedings2214-7853.

[72] Sputtering [SubsTech], (n.d.). https://www.substech.com/dokuwiki/doku.php?id=sputtering (accessed July 22, 2020).

[73] Sputter Coating Technologies: Direct Current (DC) Sputtering, (n.d.). https://www.sputtertargets.net/sputter-coating-technologies-direct-current-dc-sputtering.html (accessed September 7, 2020).

[74] Encyclopedia of Tribology, Springer US, 2013. https://doi.org/10.1007/978-0-387-92897-5.

[75] I.V. Tudose, F. Comanescu, P. Pascariu, S. Bucur, L. Rusen, F. Iacomi, E. Koudoumas, M.P. Suchea, Chemical and physical methods for multifunctional nanostructured interface fabrication, in: Functional Nanostructured Interfaces for Environmental and Biomedical Applications, Elsevier, 2019: pp. 15–26. https://doi.org/10.1016/B978-0-12-814401-5.00002-5.

[76] RF-Sputtering principles - IFN Trento, (n.d.). http://www.tn.ifn.cnr.it/facilities/rf-sputtering-facility/rf-sputtering-principles (accessed July 23, 2020).

[77] Thin film technology by KL Chopra, (n.d.).

[78] The Importance of DC Self-Bias Voltage in Plasma Applications, (n.d.). https://www.palomartechnologies.com/blog/the-importance-of-dc-self-bias-voltage-in-plasma-applications (accessed July 29, 2020).

[79] Advances In RF Sputtering - Aultimut, (n.d.). http://www.aultimut.com/technologies-2/plasma-processes/advances-in-rf-sputtering/ (accessed September 7, 2020).

[80] Magnetron Sputtering Overview, (n.d.). https://angstromengineering.com/tech/magnetron-sputtering/ (accessed July 29, 2020).

[81] D. Maurya, A. Sardarinejad, K. Alameh, Recent Developments in R.F. Magnetron Sputtered Thin Films for pH Sensing Applications—An Overview, Coatings. 4 (2014) 756–771. https://doi.org/10.3390/coatings4040756.

[82] R. Surmenev, A. Vladescu, M. Surmeneva, A. Ivanova, M. Braic, I. Grubova, C.M. Cotrut, Radio Frequency Magnetron Sputter Deposition as a Tool for Surface Modification of Medical Implants, in: Modern Technologies for Creating the Thin-Film Systems and Coatings, InTech, 2017. https://doi.org/10.5772/66396.

[83] D. Kefallinou, K. Ellinas, T. Speliotis, K. Stamatakis, E. Gogolides, A. Tserepi, Optimization of antibacterial properties of “hybrid” metal-sputtered superhydrophobic surfaces, Coatings. 10 (2020). https://doi.org/10.3390/coatings10010025.

[84] T.S. Demina, M.S. Piskarev, O.A. Romanova, A.K. Gatin, B.R. Senatulin, E.A. Skryleva, T.M. Zharikova, A.B. Gilman, A.A. Kuznetsov, T.A. Akopova, P.S. Timashev, Plasma treatment of poly(ethylene terephthalate) films and chitosan deposition: DC-vs. AC-discharge, Materials. 13 (2020). https://doi.org/10.3390/ma13030508.

[85] M. Benelmekki, A. Erbe, Nanostructured thin films–background, preparation and relation to the technological revolution of the 21st century, in: Frontiers of Nanoscience, Elsevier Ltd, 2019: pp. 1–34. https://doi.org/10.1016/B978-0-08-102572-7.00001-5.

[86] A.I. Safonov, D. v. Kuznetsov, A.S. Surtaev, Fabrication of Hydrophobic Coated Tubes for Boiling Heat Transfer Enhancement, Heat Transfer Engineering. (2020) 1–14. https://doi.org/10.1080/01457632.2020.1794632.

[87] A.M. Kietzig, M.N. Mirvakili, S. Kamal, P. Englezos, S.G. Hatzikiriakos, Laser-patterned super-hydrophobic pure metallic substrates: Cassie to Wenzel wetting transitions, Journal of Adhesion Science and Technology. 25 (2012) 2789–2809. https://doi.org/10.1163/016942410X549988.

[88] A.Y. Vorobyev, C. Guo, Multifunctional surfaces produced by femtosecond laser pulses, Journal of Applied Physics. 117 (2015). https://doi.org/10.1063/1.4905616.

[89] Ion Beam Sputtering - an overview | ScienceDirect Topics, (n.d.). https://www.sciencedirect.com/topics/chemistry/ion-beam-sputtering (accessed September 1, 2020).

[90] M.Y. Ali, W. Hung, F. Yongqi, A review of focused ion beam sputtering, International Journal of Precision Engineering and Manufacturing. 11 (2010) 157–170. https://doi.org/10.1007/s12541-010-0019-y.

[91] Y.-W. Park, Y.-J. Jo, I.-T. Hwang, J.-H. Choi, superhydrophobic-100keV-PFA, Journal of Radiation Industry. 6 (2012) 323–328.

[92] U.B. Singh, D.C. Agarwal, S.A. Khan, M. Kumar, A. Tripathi, R. Singhal, B.K. Panigrahi, D.K. Avasthi, Engineering of hydrophilic and plasmonic properties of Ag thin film by atom beam irradiation, Applied Surface Science. 258 (2011) 1464–1469. https://doi.org/10.1016/j.apsusc.2011.09.105.

[93] K.D. Weltmann, E. Kindel, R. Brandenburg, C. Meyer, R. Bussiahn, C. Wilke, T. von Woedtke, Atmospheric pressure plasma jet for medical therapy: Plasma parameters and risk estimation, Contributions to Plasma Physics. 49 (2009) 631–640. https://doi.org/10.1002/ctpp.200910067.

[94] E. Amanatides, D. Mataras, Modeling and Diagnostics of He Discharges for Treatment of Polymers, in: Advanced Plasma Technology, Wiley-VCH Verlag GmbH & Co. KGaA, Weinheim, Germany, 2008: pp. 55–74. https://doi.org/10.1002/9783527622184.ch4.

[95] P.K. Chu, S. Qin, C. Chan, N.W. Cheung, L.A. Larson, Plasma immersion ion implantation - A fledgling technique for semiconductor processing, Materials Science and Engineering R: Reports. 17 (1996) 207–280. https://doi.org/10.1016/S0927-796X(96)00194-5.

[96] C. Tendero, C. Tixier, P. Tristant, J. Desmaison, P. Leprince, Atmospheric pressure plasmas: A review, Spectrochimica Acta - Part B Atomic Spectroscopy. 61 (2006) 2–30. https://doi.org/10.1016/j.sab.2005.10.003.

[97] R.K. Sahoo, A. Das, S.K. Singh, B.K. Mishra, Synthesis of surface modified SiC superhydrophobic coating on stainless steel surface by thermal plasma evaporation method, Surface and Coatings Technology. 307 (2016) 476–483. https://doi.org/10.1016/j.surfcoat.2016.09.027.

[98] J.M. Nokes, H. Sharma, R. Tu, M.Y. Kim, M. Chu, A. Siddiqui, M. Khine, Nanotextured shrink wrap superhydrophobic surfaces by argon plasma etching, Materials. 9 (2016) 1–11. https://doi.org/10.3390/ma9030196.

[99] T.J. Ko, S.J. Park, M.S. Kim, S.M. Yoon, S.J. Kim, K.H. Oh, S. Nahm, M.W. Moon, Single-step plasma-induced hierarchical structures for tunable water adhesion, Scientific Reports. 10 (2020). https://doi.org/10.1038/s41598-019-56787-z.

[100] K. v. Chauhan, D.G. Subhedar, R. Prajapati, D. Dave, Experimental investigation of wettability properties for zirconia based coatings by RF magnetron sputtering, Materials Today: Proceedings. 26 (2020) 2447–2451. https://doi.org/10.1016/j.matpr.2020.02.520.

[101] M. Minařík, E. Wrzecionko, A. Minařík, O. Grulich, P. Smolka, L. Musilová, I. Junkar, G. Primc, B. Ptošková, M. Mozetič, A. Mráček, Preparation of hierarchically structured polystyrene surfaces with superhydrophobic properties by plasma-assisted fluorination, Coatings. 9 (2019). https://doi.org/10.3390/coatings9030201.

[102] H. Ryu, J. Kim, J. Kim, D.H. Kim, Y.J. Kang, Y.J. Jang, J.H. Jeong, Enhancement of a heat transfer performance on the Al6061 surface using microstructures and fluorine-doped diamond-like carbon (F-DLC) coating, International Journal of Heat and Mass Transfer. 148 (2020). https://doi.org/10.1016/j.ijheatmasstransfer.2019.119108.

[103] B. Subeshan, A. Usta, R. Asmatulu, Deicing and self-cleaning of plasma-treated superhydrophobic coatings on the surface of aluminum alloy sheets, Surfaces and Interfaces. 18 (2020). https://doi.org/10.1016/j.surfin.2020.100429.

[104] H. Liu, X. Wang, Z. Lan, S. Liu, Effect of tetrafluorethane and sulfur hexafluoride plasma treatment on wettability of boron nitride nano-sheets, Acta Physica Polonica A. 136 (2019) 467–473. https://doi.org/10.12693/APhysPolA.136.467.

[105] S. Orazbayev, R. Zhumadilov, A. Zhunisbekov, M. Gabdullin, Y. Yerlanuly, A. Utegenov, T. Ramazanov, Superhydrophobic carbonous surfaces production by PECVD methods, Applied Surface Science. 515 (2020). https://doi.org/10.1016/j.apsusc.2020.146050.

[106] R. Jafari, G. Momen, E. Eslami, Fabrication of icephobic aluminium surfaces by atmospheric plasma jet polymerisation, Surface Engineering. 35 (2019) 450–455. https://doi.org/10.1080/02670844.2018.1509813.

[107] A. Siddaramanna, N. Saleema, D.K. Sarkar, A versatile cost-effective and one step process to engineer ZnO superhydrophobic surfaces on Al substrate, Applied Surface Science. 311 (2014) 182–188. https://doi.org/10.1016/j.apsusc.2014.05.039.

[108] N. Sharifi, M. Pugh, C. Moreau, A. Dolatabadi, Developing hydrophobic and superhydrophobic TiO2 coatings by plasma spraying, Surface and Coatings Technology. 289 (2016) 29–36. https://doi.org/10.1016/j.surfcoat.2016.01.029.

[109] N. Sharifi, F. ben Ettouil, C. Moreau, A. Dolatabadi, M. Pugh, Engineering surface texture and hierarchical morphology of suspension plasma sprayed TiO2 coatings to control wetting behavior and superhydrophobic properties, Surface and Coatings Technology. 329 (2017) 139–148. https://doi.org/10.1016/j.surfcoat.2017.09.034.

[110] H. fan Huang, Y. qiong An, X. Hu, D. Wu, H. wei Cao, X. Zhang, J. hao Qiao, H. tao Liu, A plasma sprayed superhydrophobic coating prepared with Al@WO3 core-shell powder and photocatalytic degradation performance, Surface and Coatings Technology. 369 (2019) 105–115. https://doi.org/10.1016/j.surfcoat.2019.04.055.

[111] S. Sarbada, Y.C. Shin, Superhydrophobic contoured surfaces created on metal and polymer using a femtosecond laser, Applied Surface Science. 405 (2017) 465–475. https://doi.org/10.1016/j.apsusc.2017.02.019.

[112] J. Li, J. Xu, Z. Lian, Z. Yu, H. Yu, Fabrication of antireflection surfaces with superhydrophobic property for titanium alloy by nanosecond laser irradiation, Optics and Laser Technology. 126 (2020) 106129. https://doi.org/10.1016/j.optlastec.2020.106129.